MARTIN MARIETTA ENERGY SYSTEMS LIBRARIES

3 4456 0364222 6

DOCUMENT COLLECTION

ORNL-3046
UC-81 - Reactors-Power

MARITIME REACTOR PROJECT

ANNUAL PROGRESS REPORT

FOR PERIOD ENDING NOVEMBER 30, 1960

CONTENTS
PARTIALLY
ILLEGIBLE
DO NOT TAKE
FROM
THIS
BUILDING

OAK RIDGE NATIONAL LABORATORY
operated by
UNION CARBIDE CORPORATION
for the
U.S. ATOMIC ENERGY COMMISSION

Printed in USA. Price $1.50. Available from the

Office of Technical Services
Department of Commerce
Washington 25, D.C.

LEGAL NOTICE

This report was prepared as an account of Government sponsored work. Neither the United States, nor the Commission, nor any person acting on behalf of the Commission:

A. Makes any warranty or representation, expressed or implied, with respect to the accuracy, completeness, or usefulness of the information contained in this report, or that the use of any information, apparatus, method, or process disclosed in this report may not infringe privately owned rights; or

B. Assumes any liabilities with respect to the use of, or for damages resulting from the use of any information, apparatus, method, or process disclosed in this report.

As used in the above, "person acting on behalf of the Commission" includes any employee or contractor of the Commission, or employee of such contractor, to the extent that such employee or contractor of the Commission, or employee of such contractor prepares, disseminates, or provides access to, any information pursuant to his employment or contract with the Commission, or his employment with such contractor.

ORNL-3046

Reactors—Power
TID-4500 (15th ed.)

Contract No. W-7405-eng-26

MARITIME REACTOR PROJECT
ANNUAL PROGRESS REPORT

for Period Ending November 30, 1960

H. C. McCurdy, Reactor Division

DATE ISSUED

JAN 6 1961

OAK RIDGE NATIONAL LABORATORY
Oak Ridge, Tennessee
operated by
UNION CARBIDE CORPORATION
for the
U. S. ATOMIC ENERGY COMMISSION

MARTIN MARIETTA ENERGY SYSTEMS LIBRARIES

3 4456 0364222 6

CONTENTS

1. INTRODUCTION AND SUMMARY 1

2. N. S. SAVANNAH PROJECT — GENERAL SUPPORT 5

Shielding Survey 5

Instrument Calibration 7

Radiation Detection Instruments 9

Mobile Radiation Detection Laboratory 11

Reactor Controls 11

Analog Computer Studies 11

Examination of the N. S. Savannah Reactor Training Simulator 15

Materials Evaluation 16

Measurement of D′ for Core I Fuel Materials 16

Irradiation of Pressure-Vessel Steels 19

Waste Disposal 22

3. PRESSURIZED-WATER IN-PILE TEST LOOP 23

Design, Construction, and Operation 23

Flux Measurements 24

4. ADVANCED CORE DEVELOPMENT 40

Zircaloy Fuel-Container Studies 41

Physics 41

Zircaloy Properties 48

Fuel Development 50

Rotary Swaging of Stainless Steel-Clad UO_2 Fuel Rods 50

Fabrication of Fuel Rods by Vibratory Compaction 53

Development of Compartmented Fuel Plates 54

Irradiation Tests 58

MARITIME REACTOR PROJECT ANNUAL PROGRESS REPORT

1. INTRODUCTION AND SUMMARY

Construction of the N. S. Savannah, the first nuclear-powered cargo-passenger ship, is nearing completion at the New York Shipbuilding Corporation of Camden, New Jersey. Precritical testing of the power plant systems and components is under way. Fuel elements and control rods for the initial core are ready for installation, after having been tested in zero-power experiments in the manufacturer's critical experiment facilities. The 63-Mw(t) pressurized-water reactor and the propulsion equipment for the N. S. Savannah were supplied by The Babcock & Wilcox Company of Lynchburg, Virginia. States Marine Lines, Inc., will operate the ship following completion of sea trials by the builder.

During the present report period, the Laboratory continued to provide technical assistance to the AEC Division of Reactor Development (MAR) on certain aspects of the N. S. Savannah program. As in the past, this assistance has consisted of two general types of activities: (1) review and technical advisory services and (2) supplementary studies, experimental programs, and specialized services.

Support of the N. S. Savannah project continued to involve some design review, although there was a marked reduction in this type of activity during the current report period. Most of the detailed review effort was concerned with core II design, fabrication specifications, and test work. Assistance in the development of the N. S. Savannah test program was provided by an ORNL engineer who was assigned to the AEC-MARAD group at the Shipyard from September 1959, until December 1960. The ORNL Neutron Physics Division made preparations to measure dose levels in passenger and crew areas when the reactor is initially operated at significant power. Instrumentation for this purpose was designed, assembled, and calibrated.

Experimental measurements were made of the pseudo-diffusion coefficient, D', of N. S. Savannah core I fuel pellets produced by The

Babcock & Wilcox Company. This property is used for characterizing the fission-gas retention properties of UO_2 fuel pellets. Results of the measurements indicate that the N. S. Savannah oxide can be expected to compare favorably with other oxide fuels. Charpy V-notch impact specimens made from type A212, grade B steel scrap from the N. S. Savannah reactor vessel upper closure head were irradiated in the Maritime pressurized-water loop in the Oak Ridge Research Reactor. The range of fast-neutron dosage was designed to bracket the expected maximum dose which the N. S. Savannah reactor vessel will receive during its 20-year life, but the dose rate was accelerated by about two orders of magnitude.

Waste disposal studies which were aimed at the development of improved techniques for sea disposal of radioactive wastes from nuclear merchant ships were terminated. A report was issued describing investigations of procedures for fixation of ion-exchange resins in concrete to facilitate disposal.

The ORNL Inspection Engineering Department continued to act as an inspection agency for the AEC, witnessing inspections and tests during fabrication of nuclear components. Inspection of equipment for the initial N. S. Savannah installation was completed, and assistance was provided in the inspection of replacement parts and a prototype of a control drive mechanism which is under development. For part of the current report period resident inspection was provided at the Shipyard to assist the MARAD inspection group during reactor installation and at the General Electric plant in San Jose, California, during the manufacture of core II.

Construction of the Maritime pressurized-water loop in the Oak Ridge Research Reactor was completed, and operation began in December 1959. The loop has operated satisfactorily, and only minor corrections and modifications have been required. It has been used for the irradiation of carbon steel from the N. S. Savannah reactor vessel and is currently being used for testing proposed fuel materials.

With the decline of design review and N. S. Savannah support activities, increased emphasis has been placed on advanced core

development. The Laboratory's efforts are directed toward: (1) investigating the feasibility and potential benefits of replacing the present fuel container assembly with a zirconium alloy assembly and (2) the development and testing of nonsintered UO_2 fuel elements. These two features appear to offer attractive potential for achieving marked reductions in fuel cycle costs.

Substitution of Zircaloy for stainless steel fuel containers was found to have pronounced effects on core physics that were exhibited principally by a decrease in enrichment required for a given multiplication and by an appreciable increase in control rod worth. Because of the importance of core heterogeneities, it was felt that previously used calculational techniques were not adequate for evaluating the effects of the proposed change. An analytical method was devised and tested against data from several critical experiments. The comparison indicated that the calculation method successfully reproduces the effect of egg-crate material on the static multiplication factor and on control rod worth.

Work on advanced fuel materials consisted principally of metallurgical investiations of alternate fabrication methods for encapsulating UO_2 in stainless steel, viz., (1) rotary swaging, (2) vibratory compaction, and (3) compartmented fuel plates. The effect of swaging temperature on density for a constant reduction in area was determined for each of three types of commercially produced swageable UO_2. The influence of swaging temperature and total swaging reduction on the tendency of the type 304 stainless steel cladding to crack was investigated. It was found that crack-free cladding was obtained with cold reductions in area of less than 65% and at swaging temperatures of less than 600°C. Irradiation testing of swaged-UO_2 fuel rods was initiated in the Maritime pressurized-water loop. Near the end of the current report period, studies of the vibratory compaction process, which were under way at ORNL as part of another program, were extended to fuels and fuel-rod geometries of interest to the Maritime program. Equipment difficulties were encountered in the initial tests, and no valid data were obtained.

The compartmented fuel plate work consisted of investigations of methods for fabricating stainless steel fuel plates containing several individual leaktight compartments. A formed and spot-welded design for the grid assembly was found to be unsatisfactory because of difficulties with nonbonding and resultant intercompartmental leakage. These difficulties were encountered when cover sheets were bonded to the grids by either brazing or resistance welding. Two other designs are being evaluated.

2. N. S. SAVANNAH PROJECT — GENERAL SUPPORT

Shielding Survey

(T. V. Blosser)

The Oak Ridge National Laboratory has been asked to make a radiation-intensity survey of the exterior of the N. S. Savannah reactor-compartment shield. Since the radiation levels proposed for the exterior of this shield are exceptionally low, in some places as low as 0.5 rem/yr, special instrumentation and prior adjunct experiments are required.

No fast-neutron dose detectors are available which will give reliable direct measurements of the low levels expected. Consequently, it will be necessary to use an instrument of very high sensitivity, even though it has not been proved to give a response proportional to biological dose. This instrument, a specially constructed long counter, will be calibrated against the standard Hurst fast-neutron dosimeter in a fast-neutron field designed to be like that emerging from the N. S. Savannah shield. This field will be obtained by the use of shield mockups constructed for the purpose and inserted in the ORNL Bulk Shielding Facility adjacent to the reactor. These specially calibrated and modified long counters will then be used for basic measurements on the N. S. Savannah.

The general survey of the N. S. Savannah shield exterior will be carried out with gamma-ray and thermal-neutron detectors which are inherently much more sensitive than fast-neutron detectors and which will reveal regions of higher than average leakage. The instruments to be used in the shield survey have been built and are undergoing adjustments. Calibration will proceed during the next two months. The instruments will be installed in a Vanette truck which will be driven to the N. S. Savannah at dockside and hoisted aboard for use in measurements at sea.

The N. S. Savannah shield[1,2] consists of a primary shield around the reactor and a secondary shield around all the steam-producing equipment. The thicknesses of the various layers are shown in Fig. 2.1. The innermost region of the primary shield consists of alternate layers of

[1]W. R. Smith and M. A. Turner, "Nuclear Merchant Ship Reactor Shield Design Summary Report," BAW-1144-1, Aug. 1, 1959.

[2]W. R. Smith and M. A. Turner, "Design of NMSR Primary Shield," BAW-1101, April 1958.

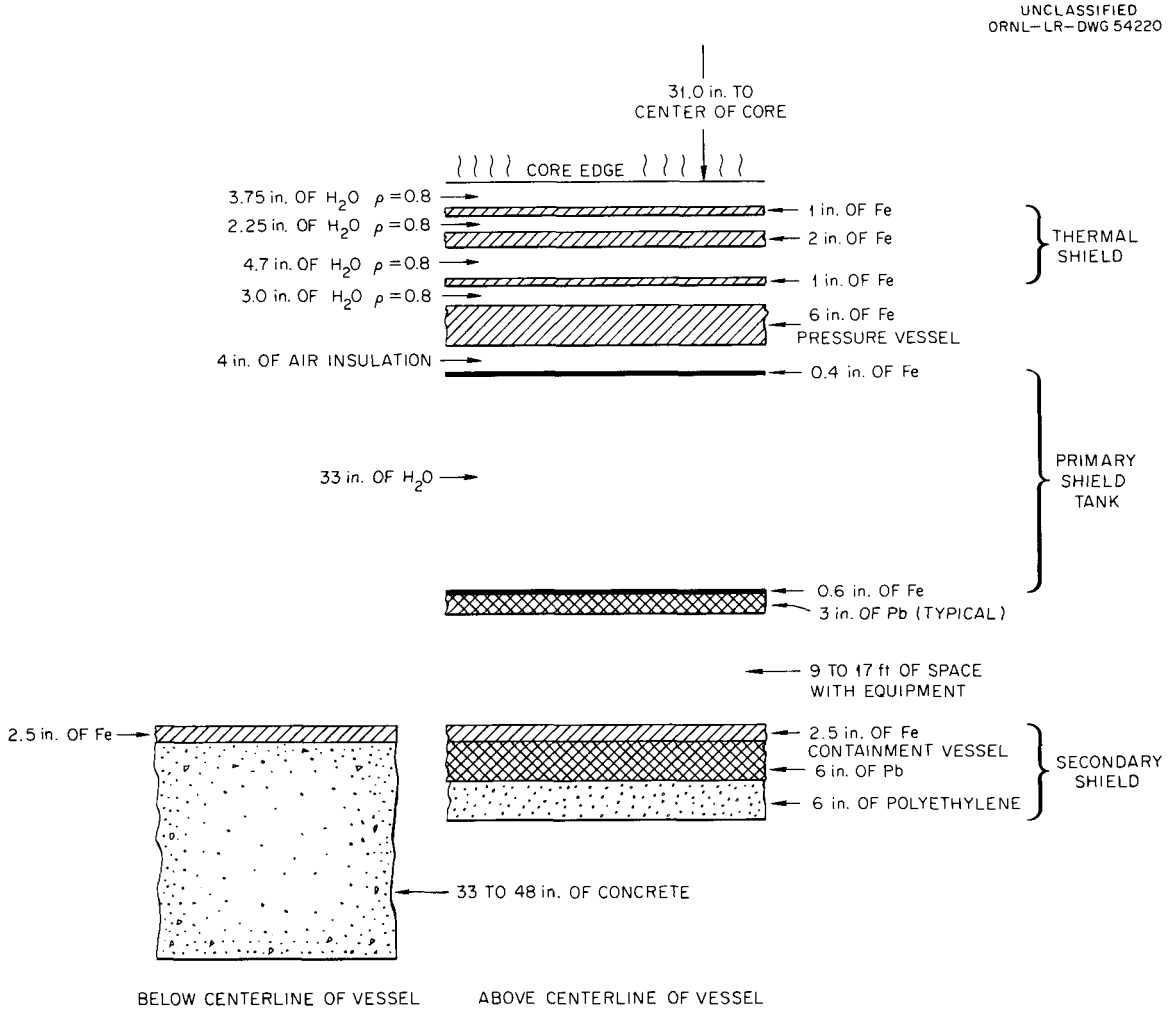

Fig. 2.1. Schematic Cross Section at Mid-Plane of N. S. Savannah Reactor Shield.

iron and water that make up the thermal shield and the 6-in.-thick pressure vessel. Exterior to this is the 33-in.-thick water-filled primary shield tank, followed by a layer of lead on the tank exterior that varies in thickness from 1 to 4 in. Exterior to this primary shield, various pieces of steam-production equipment are installed, including boilers, pumps, demineralizers, etc. The core, thermal shield, pressure vessel, primary shield, and steam-production equipment are all enclosed in a 2.5-in.-thick containment vessel that is a horizontal steel cylinder 35 ft in diameter. The vessel has hemispherical ends, giving a total length of 50 ft 6 in. Exterior to this vessel, additional shielding material comprises the secondary shield. Above the mid-plane the secondary shield consists of a layer of lead that varies in thickness between 5 and 6 in., followed by a minimum of 8 in. of polyethylene. Below the mid-plane, concrete of various thicknesses (33 to 43 in.) is used. Fore and aft on the hemispherical sections, the concrete is made with an ilmenite aggregate; ordinary concrete is used on the cylindrical sides. Collision mats consisting of alternate layers of redwood and steel displace some of the concrete shielding in this region. The dose rates which comprise the design criteria for the biological shield are given in Table 2.1 (ref. 3).

Instrument Calibration

Gamma-ray ionization chambers and anthracene scintillation detectors, as well as fast-neutron dosimeters and thermal-neutron detectors, will be calibrated by standard techniques. The detection of extremely low levels of fast neutrons is to be accomplished, as mentioned above, with a special fast-neutron detector, the response of which is designed to (but not yet proven to) match the biological response of human tissue to neutrons of various energies. Experiments are planned with the ORNL Van de Graaff generator to determine whether the design goal has been achieved. In addition, as an over-all calibration of this instrument,

---

[3]G. E. Kulynych, "Nuclear Merchant Ship Reactor Final Safeguard Report," BAW-1164, Vol. I, March 1960.

Table 2.1. Design Dose Rates for the N. S. Savannah Shield

Location	Operating Conditions	Type of Access	Control Area	Design Dose Rate
Access spaces outside secondary shield (passenger spaces)	Full power	Normal	Yes (initial operations)	5.0 rem/yr
			No (ultimately)	0.5 rem/yr
Access spaces outside secondary shield (crew spaces)	Full power	Normal	Yes	5.0 rem/yr
Cargo holds	One-fifth of full power	Limited	Yes	0.5 rem/yr
Inside containment vessel	Reactor operating	Not permitted	Yes	
	Reactor shut down 1/2 hr or longer; no fission products in primary loops	Limited	Yes	200 mr/hr
Locations occupied during fuel transfer operations	Reactor shut down 3 days or longer	Limited	Yes	200 mr/hr (transient conditions)
				10 mr/hr (continuing conditions)

its response will be compared to that of the Hurst fast-neutron dosimeter in radiation fields which are similar in energy spectrum to those to be expected on the N. S. Savannah. In order to match the spectrum leaving the secondary shield, the mockups shown in Fig. 2.2 will be installed in the Bulk Shielding Facility adjacent to the reactor. In order to compare the dosimeter, which is of low sensitivity, and the long counter, for which the sensitivity is considerably greater, it may be necessary to operate the reactor at widely different power levels and to relate the doses to the power calibration of the reactor. If it is impossible because of low intensity to obtain a reliable reading of the fast-neutron dosimeter with the mockup as pictured, the inner regions of the shield mockup will be removed and the mockup foreshortened. This procedure may sacrifice in small measure the correspondence of mockup to actual shield, but the leakage spectrum should not change greatly, since it will be determined principally by the outermost regions of the shield.

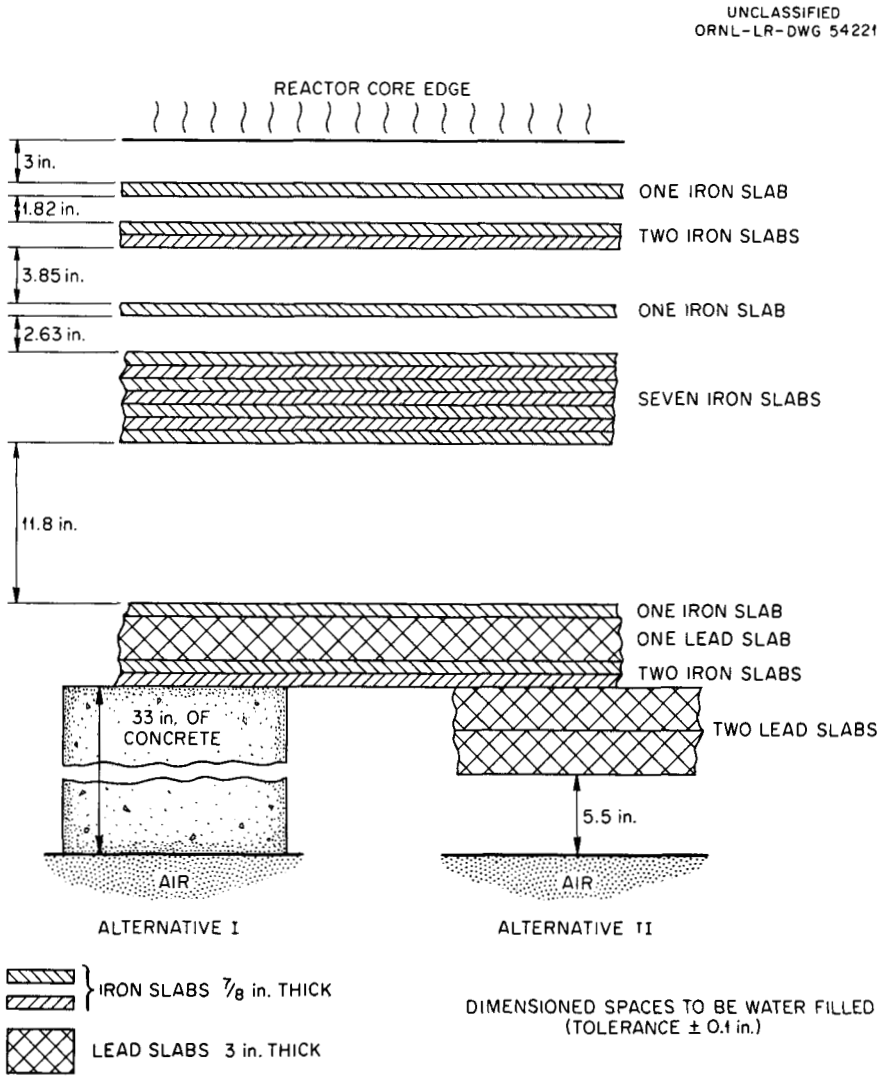

Fig. 2.2. Schematic Cross Section of BSF Mockup of Mid-Plane of N. S. Savannah Reactor Shield.

Radiation Detection Instruments

In order to evaluate the biological effectiveness of a shield, it is necessary to use detectors that can be calibrated to give the radiation dose which would be important to human tissue. The radiation dose is obtained separately for gamma rays, fast neutrons, thermal neutrons, and intermediate energy neutrons. The biological dose from gamma rays and fast neutrons is proportional to the energy loss by the radiation

in passing through tissue. Accordingly, the gamma-ray and fast-neutron detectors should have absorptive characteristics similar to human tissue. However, the biological dose from thermal neutrons is proportional to the number of neutrons absorbed in the body, and a flux-measuring instrument will be used for this component. The detectors used in this survey essentially fulfill the above-mentioned requirements for estimating radiation doses. The specific detectors which have been chosen are described in the following paragraphs.

Gamma-Ray Detectors. The standard instrument that will be used for gamma-ray detection will be a 900-cm^3, CO_2-filled, carbon-walled, ionization chamber. Since the sensitivity of this instrument is such that it can be used reliably only to measure fields of 10 mr/hr or greater, it will be used principally for intercalibration with a more sensitive instrument (described below), although it may be used on occasion on shipboard for measuring the higher fields.

Anthracene scintillation detectors, which are similar to tissue in energy-deposition characteristics, will be used as a secondary standard in measuring tissue gamma-ray doses. The measured dose is proportional to the total energy deposition of the secondary electrons that gamma rays produce in the scintillator. The crystal has been encased by a small thickness (0.3 cm) of Lucite to establish secondary electron equilibrium in an effort to match the energy response of the crystal to that of tissue. Monoenergetic gamma-ray sources of various energies will be used to determine the degree of matching that has been achieved. Finally, this instrument will also be calibrated against the standard ionization chamber in a typical radiation field which will be obtained with the mockups shown in Fig. 2.2. Thus calibrated, however, this instrument can be used to measure fields as low as 0.01 mr/hr with a pulse-counting technique. For considerably higher fields the photocurrent will be measured.

Fast-Neutron Detectors. The standard fast-neutron detection instrument will be the Hurst fast-neutron dosimeter, which is a recoil-proton proportional counter with an energy integrating circuit. This

instrument can be used only to measure fast-neutron dose rates in excess of 0.10 mrad/hr.

A modified long counter will also be used for fast-neutron dose indication aboard ship. As mentioned previously, it will be calibrated in a mocked up typical fast-neutron spectrum.

Thermal-Neutron Detectors. The standard BF_3 proportional counters presently used at ORNL will be utilized to measure thermal-neutron fluxes both in the mockup experiments and on shipboard. These instruments will be used throughout the ship to search for regions of unexpected radiation leakage.

Mobile Radiation Detection Laboratory

The radiation detection instruments and field-calibrated sources will be mounted in a Vanette truck, as shown in Fig. 2.3. The inside of the Vanette truck is shown in Figs. 2.4 and 2.5. The large cylinder in the foreground of Fig. 2.4 is a paraffin shield used to enclose a fast-neutron source. This shield is recessed to accommodate fast-neutron detectors for in-place calibration. Each instrument will consist of a detector-preamplifier unit, 250 ft of coaxial cable, and, mounted in the Vanette truck, a linear amplifier and scaling unit. The electric power required for the instruments and air-conditioning is to be supplied from the ship.

Reactor Controls

(E. R. Mann)

Analog Computer Studies

The ORNL Analog Computer was utilized for an examination of the Babcock & Wilcox closed-loop controller for the primary coolant system and of an alternate proposed controller. It was concluded that the B&W controller should work satisfactorily provided the detailed engineering and fabrication are adequate, although a much faster maximum rod speed would be desirable to extend the effective range of the controller.

Fig. 2.3. Vanette Truck Housing for Instruments for N. S. Savannah Shield Survey.

The alternate controller used the error signal

$$\epsilon = T_H(t - \tau) + K_1 \frac{d}{dt} T_H(t - \tau) - K_2 F_s - \overline{T}_{Ref} \quad , \tag{1}$$

where $T_H(t - \tau)$ is the water temperature at the hottest point in the system, as measured by a temperature sensor with a time constant of τ in seconds; K_1 is a constant with the dimensions of seconds; K_2 is also a constant evaluated at design conditions from the relation

$$K_2 = \frac{T_H - \overline{T}_{Ref}}{F_s} \quad , \tag{2}$$

Fig. 2.4. Instruments Mounted on Left Side of Vanette Truck (View from Rear).

where F_s is steam flow in compatible units and $\overline{T}_{Ref}$ is the set point average temperature of the primary coolant.

The alternate controller was the "on-off" type, with a dead-band of 1°F. Control rod velocity was adjustable in the simulation with a maximum rate of change in δk from the rods of ±1.5% per minute. The maximum δk assigned to the controller was adjustable.

The analysis showed that for a fuel temperature coefficient of either $-1 \times 10^{-5}/°F$ or $-2 \times 10^{-5}/°F$ the system was unstable for a temperature-sensor time-constant, τ, of 10 sec. The system could be stabilized when τ was equal to 2.5 sec for either value of the fuel coefficient. The power overshoot both during a transient and in stable operation was sensitive to rod speeds.

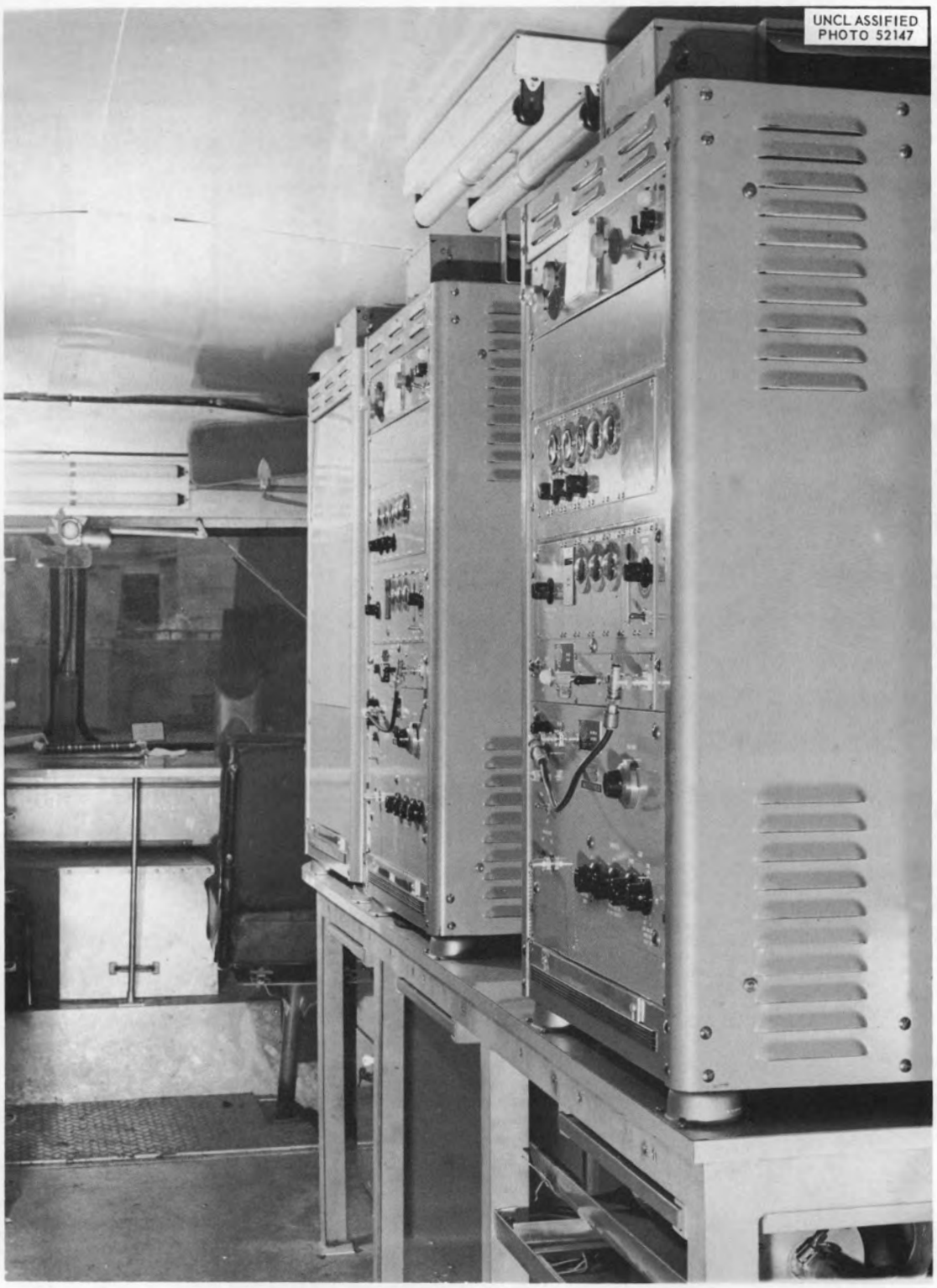

Fig. 2.5. Instruments Mounted on Right Side of Vanette Truck (View from Rear).

It was concluded that the alternate controller might be acceptable if care were taken to determine exactly what the controller was supposed to do, what the reactor power coefficient was initially, what it was likely to be as the power density shifted in the reactor during operation, and that the error signal with no flux component would not rip the safety system in positive transients. It is felt, however, that for the initial installation, the Babcock & Wilcox controller is probably preferable, since the reactor power coefficient will not be known for some time and the Babcock & Wilcox controller can be adjusted over a wide range of possible power coefficients, if necessary. Once the power coefficient is determined, it is probable that a more simple controller would perform equally well.

Examination of the N. S. Savannah Reactor Training Simulator

The N. S. Savannah training simulator was extensively revised following a previous review[4] and was installed in the Engineering Building of Lynchburg College, Lynchburg, Virginia. Performance was witnessed by ORNL personnel during the 50-hr acceptance test of the installation. Except for an occasional multiplier instability in one or two range-of-variable tests, the training simulator performed very well in all drift tests. These and other tests which were made indicated that, with the possible exception of the steam dump feature, the simulation is probably as accurate as can be expected until the plant itself is operated. When experimental data, such as the magnitude of the power coefficient, are available from the actual plant to replace design data, adjustments can be made on the training simulator so that it will perform more nearly like the N. S. Savannah.

---

[4]"Maritime Reactor Project Ann. Prog. Rep. Nov. 30, 1959," ORNL-2865, p. 10.

Materials Evaluation

Measurement of D′ for Core I Fuel Materials (J. L. Scott, W. C. Thurber, D. F. Toner)

One of the techniques currently used for characterizing the fission-gas retention properties of UO_2 fuel pellets is measurement of the noble gas diffusion parameter D′, where $D' = D/a^2$. In this relation, D is the conventional diffusion coefficient (cm^2/sec) and a is the diffusion path length (cm). This path length is a measure of the distance through which the gaseous fission products xenon and krypton must diffuse before being released from the fuel body to the external system. Since the path length is a difficult parameter to determine, the experimental results are interpreted in terms of D′.

In order to measure D′, a small fragment of UO_2 containing approximately 5 mg of U^{235} is irradiated at a low temperature for 20 to 40 hr. After irradiation the sample is allowed to decay for one week and is then placed in a high-temperature furnace where the fission gases are allowed to diffuse from the fuel. The evolved gases are adsorbed in refrigerated charcoal bulbs and counted for Xe^{133}. Sampling is conducted at various time intervals and at various temperatures. By measuring the fraction of gas released, f, in a given time, t, the diffusion parameter D′ may be calculated from the relation

$$f = 3.39\ (D't)^{1/2} \qquad \text{for } f < 0.10 \quad .$$

Studies conducted as part of the ORNL gas-cooled reactor program have shown that the D′ values measured after such short irradiations correlate reasonably well with D′ values generated in fuel capsules irradiated to burnups of approximately 16 000 Mwd/MT.

In order to determine D′ for the fuel pellets produced for core I of the N. S. Savannah reactor, a group of 20 pellets was supplied to ORNL by The Babcock & Wilcox Company. Ten of the pellets were manufactured from virgin 4.6% enriched UO_2. These pellets were sintered for 5 hr at 1630°C. The remaining ten pellets were manufactured from recycled 4.2%

enriched UO_2 fuel. Recycling consisted of oxidizing rejected pellets to U_3O_8, reducing the powder to UO_2 by heating in H_2 at 790°C, and finally repressing the oxide into pellets. The pellets containing recycled powder were sintered at 1500°C for 5 hr. Pertinent data on these two types of pellets are presented in Table 2.2. The impurity concentrations, as determined by complete dissolution of one pellet from each group, are noted in Table 2.3. Also listed are the results of the vendor's analyses of the as-supplied powder.

Results of D′ measurements at 1400 and 1800°C for one sample from each group are summarized in Table 2.4. Comparison of the data obtained at 1400°C with the data obtained at the same temperature for fuel from other sources[5] indicates that the D′ values for the core I fuel are midway within the range of observed values (10^{-14} to 10^{-10} sec^{-1}). Analyses of results from diffusion tests in which the fuel sintering temperature was exceeded (e.g., the 1800°C data) indicate much higher D′ values than would be predicted from a plot of log D′ vs 1/T. The source of this deviation is not known at the present time. Consequently, it is assumed for purposes of calculation that all fission gases are released in areas where the fuel temperature exceeds approximately 1600°C.

---

[5]"GCR Quar. Prog. Rep. June 30, 1960," ORNL-2964, p. 90.

Table 2.2. Properties of Core I UO_2 Pellets Received for Fission-Gas Release Measurements

Identification		Enrichment (%)	Measured Density (g/cm^3)		BET Surface Area (cm^2/g)	Oxygen-to-Uranium Ratio	Uranium Content (wt %)
Inspection Batch No.	CYT-ORL Transfer No.		Bulk	CCl_4 Immersion			
50	1423	4.60	10.06	10.07	58.0	2.0093	87.98
51	1423	4.19	10.02	9.96	18.9	2.0018	88.00

Table 2.3. Impurities in UO_2 Pellets Received for Fission-Gas Release Measurements

Impurity	Quantity of Impurity Found (ppm)			
	Batch No. 50		Batch No. 51	
	ORNL	Vendor	ORNL	Vendor
C	200		200	
N	465		25	
F	31	140	11	50
Si	<10		10	
Ni	30	20	25	40
Fe	30	80	65	100
Cr	15	20	15	30
Cu	2	0.5	4	1
Pb	<6		<0.5	
Sn	<3		<3	
B	<0.6	0.2	<0.5	0.2
Cd	<23	0.2	<20	<0.2
Ag	<3	1	<2	<0.01
Eu		<0.4		<0.4
Dy		0.7		<0.4
Gd		<0.4		<0.4
Sm		<0.4		<0.4

Table 2.4. Values of the Release Rate Parameter, D′, for Release of Gaseous Fission Products from Core I Fuel Pellets

Batch No.	Sample No.	Total Test Time (hr)	Test Temperature (°C)	Total Fraction of Gas Released	Release Rate Parameter D′ (sec^{-1})
50	6	6	1400	5.6×10^{-3}	2.8×10^{-11}
		6	1800	1.5×10^{-1}	1.5×10^{-7}
51	5	1.5	1400	1.2×10^{-3}	7.0×10^{-12}
		6	1800	6.5×10^{-2}	5×10^{-8}

Irradiation of Pressure-Vessel Steels (V. O. Haynes, W. C. Thurber)

Irradiations have been completed of groups of pressure-vessel steel specimens at anticipated N. S. Savannah reactor pressure vessel operating temperatures. The integrated dose to the specimens bracketed the 1.5×10^{19} neutrons/cm^2 dose (>1 Mev) expected for the N. S. Savannah reactor vessel in 20 years.

Four eight-sample groups of full-size Charpy-V notch impact specimens were irradiated during one reactor cycle in the pressurized-water loop of the ORR. The specimens, which were machined from type A212, grade B scrap remaining from fabrication of the upper closure head of the N. S. Savannah pressure vessel, had the Charpy-V notch perpendicular to the rolling plane. Monitoring of the dose was accomplished by simultaneous exposure of high-purity nickel wires with the specimens at each location. Each group of the specimens was sealed with the nickel wires in a thin, tightly fitting stainless steel can. Components for a typical experiment are shown in Fig. 2.6. Two cans, connected by a 3/8-in.-diam rod, were inserted in each leg of the loop and exposed to the doses shown in Table 2.5 at a nominal temperature of 500°F. An assembled group of specimens may be seen in Fig. 2.7.

Table 2.5. Charpy Impact Specimen Dose

Specimen Group	Specimen No.	Neutron Dose (neutrons/cm^2 at >1 Mev)
1	A1, B1, C1, D1	4.1×10^{18}
	A2, B2, C2, D2	4.6×10^{18}
2	A3, B3, C3, D3	9.8×10^{18}
	A4, B4, C4, D4	9.7×10^{18}
3	N1, O1, P1, R1	9.9×10^{18}
	N2, O2, P2, R2	1.3×10^{19}
4	N3, O3, P3, R3	2.3×10^{19}
	N4, O4, P4, R4	2.4×10^{19}

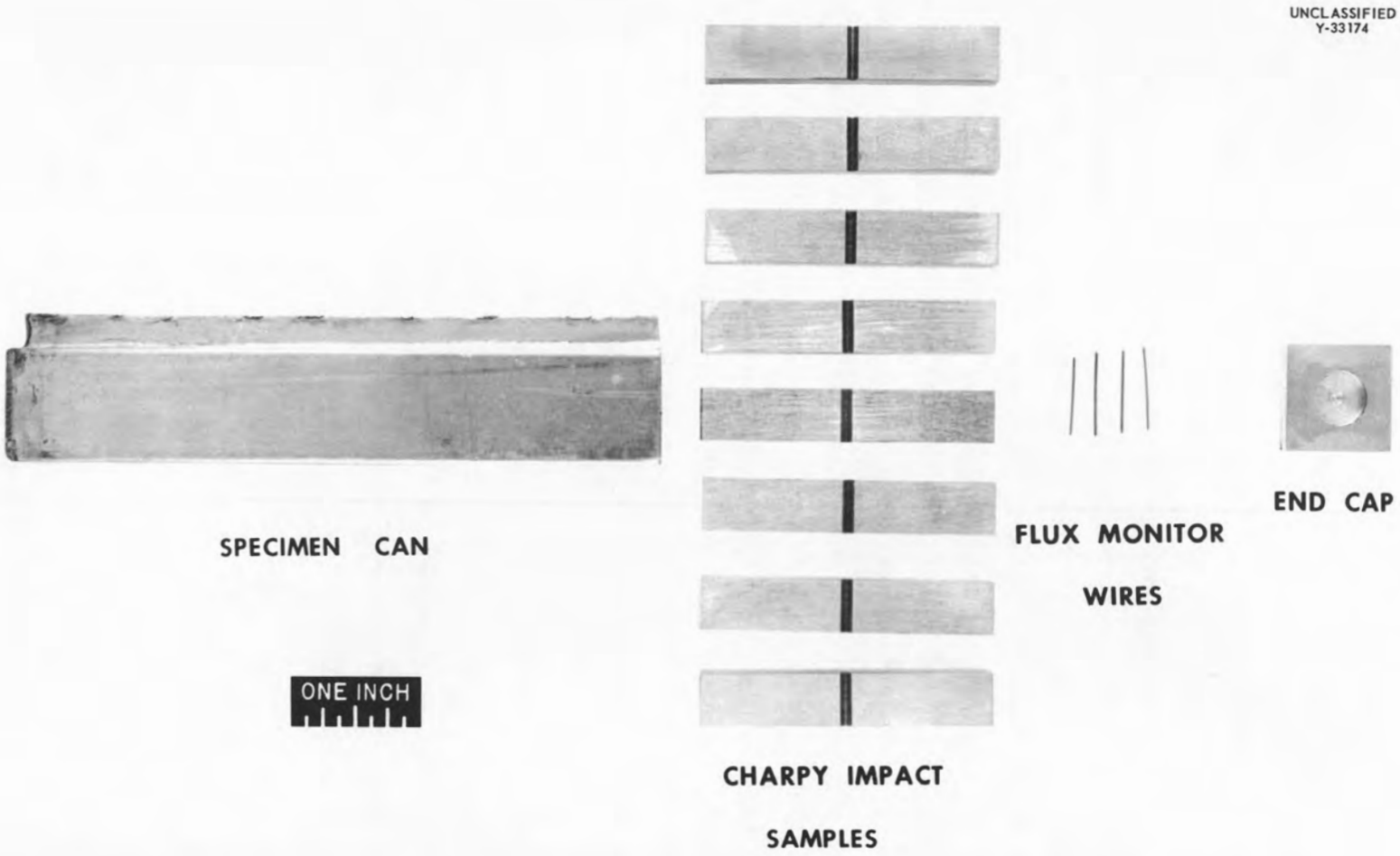

Fig. 2.6. Components for Assembly Used in Irradiation of Charpy Impact Specimens of Pressure-Vessel Steel.

Fig. 2.7. Assembled Apparatus for Irradiation of Impact Specimens of Pressure-Vessel Steel.

A set of control specimens was given an identical heat treatment out-of-pile (i.e., 23 days at 500°F). The irradiated specimens have been removed from the loop and will be stored until a hot-cell facility is available.

The change in the NDT temperature of the specimens will be determined. Because of the accelerated dose rate (two orders of magnitude higher than that predicted for the N. S. Savannah), source of the material, lack of stress in the material, absence of heat-affected zones, minor difference in irradiation temperature from the vessel-service temperature, and other factors, it is not clear how meaningful an interpretation of the results can be in terms of the N. S. Savannah reactor vessel.

Waste Disposal

Studies for improving techniques for sea disposal of radioactive wastes from nuclear merchant ships were terminated during the current report period. A report[6] was issued describing investigations of procedures for fixation of ion-exchange resins in concrete to facilitate disposal.

A mixture of two parts of portland cement, one part of resin, and one part of water was found to be optimum for the fixation of nuclear-reactor-system demineralizer resins in cement. A concrete block prepared by this receipt showed only 0.44% of the gross gamma activity leached after 2540 hr of contact with simulated sea water. The data indicated that little or no further leaching would occur.

---

[6]R. R. Holcomb, "Maritime Reactor Waste Disposal Studies: Solidification of Ion-Exchange Resin with Portland Cement for Radioactive Waste Disposal," ORNL-2899 (August 10, 1960).

3. PRESSURIZED-WATER IN-PILE TEST LOOP

Design, Construction, and Operation

(I. T. Dudley)

Design and construction of the pressurized-water loop were described previously.[1,2] Construction was completed in November 1959, and operation began in early December of that year.

Photographs made before the construction work was completed were shown in previous reports,[1,2] and photographs of the completed loop are presented here. Figure 3.1 is a simplified flow diagram of the loop. Figure 3.2 is a cutaway drawing of the pressurized-water loop installed in the ORR. Figures 3.3 and 3.4 illustrate the equipment arrangement in the basement of the ORR. A view of the operating area may be seen in Fig. 3.5. The loop makeup system is shown in Fig. 3.6. Figure 3.7 is a view of the ORR pool which shows the upper end of the in-pile section and the in-pool piping vacuum jacket. A view of the three hermetically sealed Westinghouse pumps may be seen in Fig. 3.8. The surge tank is shown in Fig. 3.9. The water-cooled heat exchanger and a section of line heaters mounted overhead may be seen in Fig. 3.10. Figure 3.11 is a view of the out-of-pile test section. Upper ends of three of the four shielded ion-exchange columns and a portion of the transmitter rack may be seen in Fig. 3.12.

The loop has been in operation since December, and only minor modifications have been found to be necessary. A monitor to detect fission-product activity has been added to the reactor cooling-water system, and a standby makeup pump has been installed. The battery-powered emergency motor-generator circuits have been reworked for increased reliability.

---

[1] "Maritime Reactor Project Ann. Prog. Rep. Nov. 30, 1958," ORNL-2657, p. 10.

[2] "Maritime Reactor Project Ann. Prog. Rep. Nov. 30, 1959," ORNL-2865, p. 17.

During the period that this test facility has been in operation the most objectionable difficulties have been a few reactor setbacks caused by malfunctioning of electronically operated temperature-monitoring safety instruments. All safety controls are designed for fail-safe operation. The rate of these incidents is normal; however, efforts are being made to reduce such instrument failures to a minimum by exercising special preventative maintenance procedures.

Flux Measurements

(V. O. Haynes)

The pressurized-water loop occupies lattice positions A-1 and A-2 of the ORR and provides a 1 1/2-in.-diam experimental region in each of these lattice positions through most of the axial ORR core length. Fast-flux measurements have been made at two locations in the A-2 loop position. The monitors used were high-purity nickel wires and sulfur encapsulated in quartz tubes. The nickel monitors were short lengths (3/4 and 2 in.) of 0.020-in.-diam wire. The 2-in. lengths were supported with their axes parallel to the ORR core axis and were located at two axial positions. The 3/4-in. lengths were located near the axial core centerline and were supported in such a manner that the axis of one pointed toward the ORR core center and the axis of the other was perpendicular to the first. The sulfur monitors consisted of sulfur sealed in small-diameter quartz tubing (the sulfur powder was in a region about 0.080 in. in diameter and 1/2 in. long). All the monitors were sealed in stainless steel tubing and mounted into the assembly shown in Fig. 3.13.

Activation was accomplished at a 20-Mw ORR power level during the January 1960 cycle (cycle 20). The Co^{58} and P^{32} activities, along with sample weights, were measured by the ORNL Analytical Chemistry Division, and subsequent calculations gave the flux values listed in Table 3.1. A value of 91 mb was used for the $Ni^{58}(n,p)Co^{58}$ cross section, and a value of 65.5 mb was used for the $S^{32}(n,p)P^{32}$ cross section. The fraction of the fast flux above 1 Mev was taken as 0.69 of the total

Table 3.1. Fast-Neutron Flux in Pressurized-Water Loop in ORR

Axial Position	Neutron Flux Above 1 Mev (neutrons/cm^2·sec)	
	By Nickel Monitor	By Sulfur Monitor
9 1/2 in. above core centerline	5.3×10^{12}	4.0×10^{12}
1/2 in. below core centerline	1.2×10^{13}	1.3×10^{13}

fast flux. Two nickel samples were exposed with their axes perpendicular to each other to determine the activation dependence on orientation; the activation was shown to be insensitive to the direction of the monitor wire axis.

Concurrent with the fast-flux measurements, three stainless steel wires were activated to gain experience in predicting the thermal-neutron flux using this type of monitor. The experimental data were analyzed by estimating the amount of Co^{60} resulting from thermal-neutron activation. Previous neutron flux measurements[3] were used to arrive at an effective Co^{59} cross section. The stainless steel wires were 0.020 in. in diameter and 20 in. long. After the irradiation, these wires were cut into 1-in. segments and counted for Co^{60} activity. The axial thermal-neutron flux values based on these data are plotted in Fig. 3.14, which also gives the radial location of the wires.

[3] Ibid., p. 36.

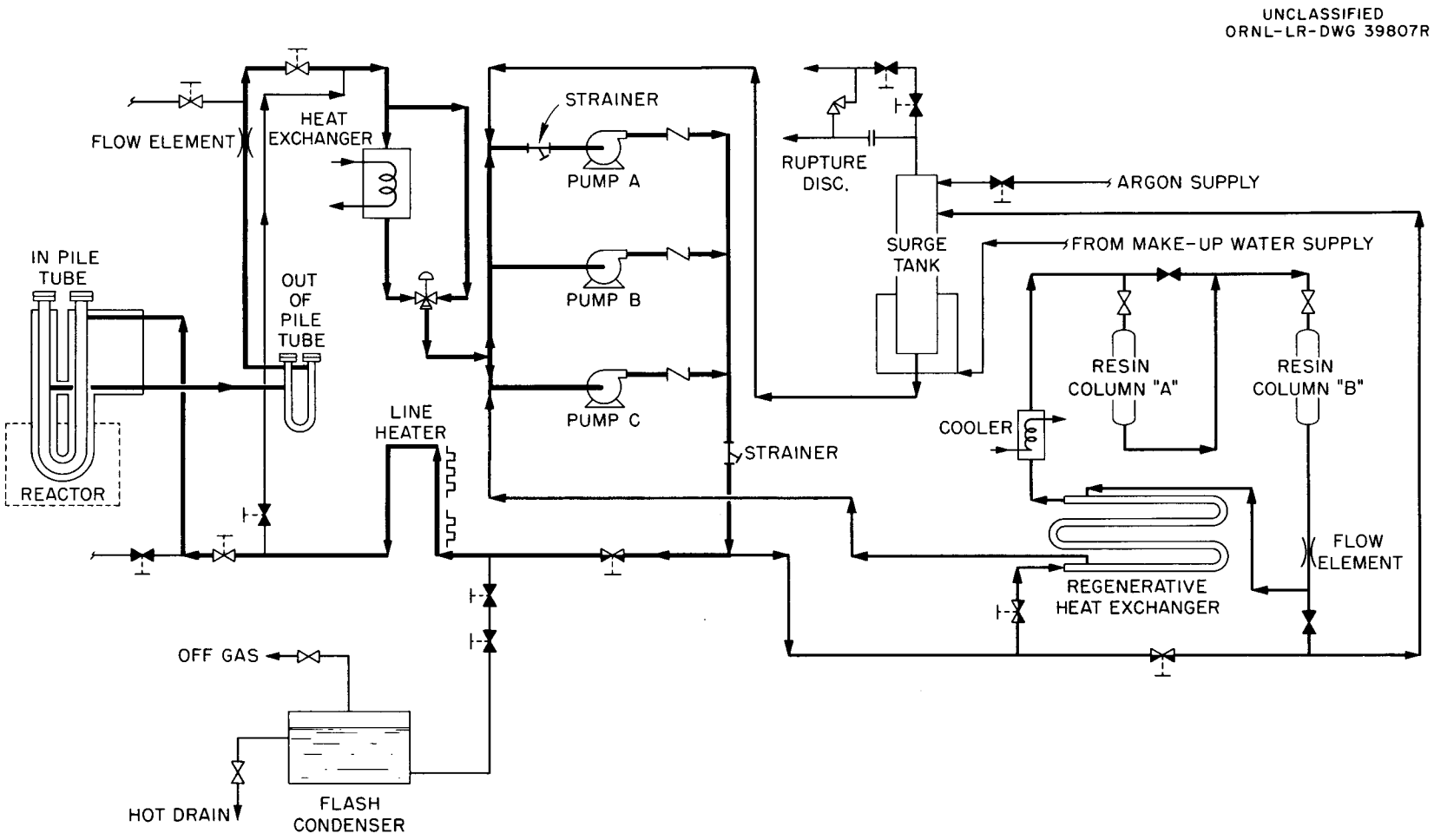

Fig. 3.1. Simplified Flow Diagram of Pressurized-Water Loop in ORR.

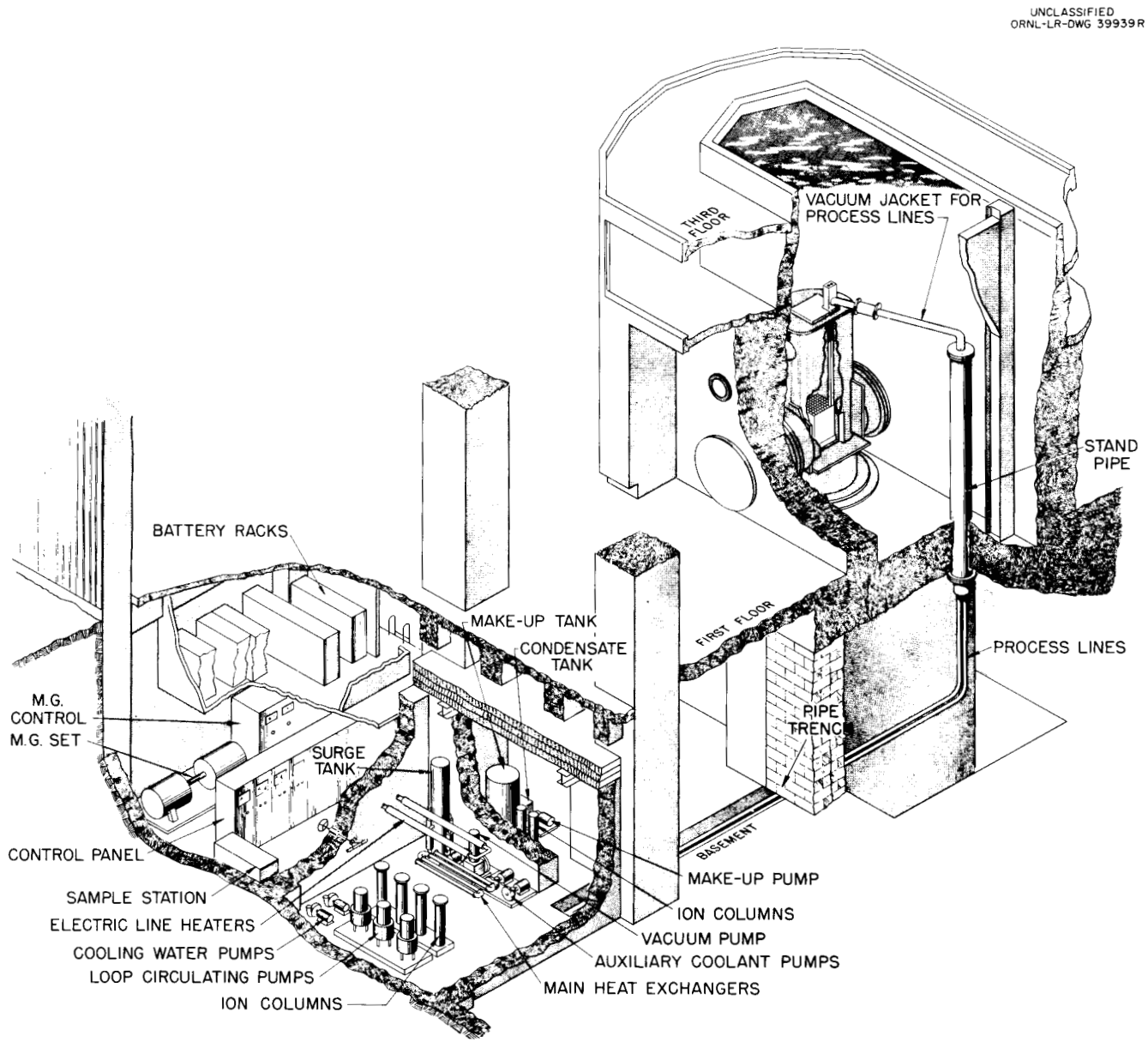

Fig. 3.2. Cutaway Drawing of Pressurized-Water Loop Installed in ORR.

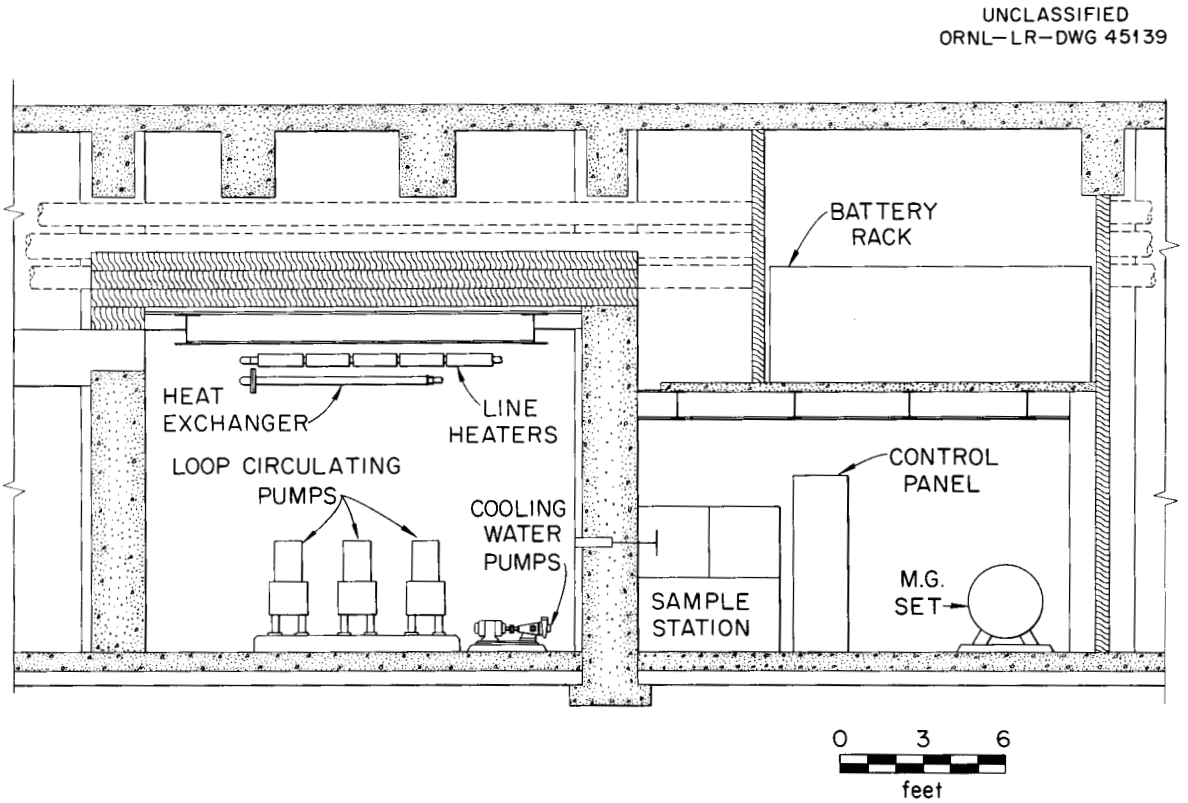

Fig. 3.3. Elevation Drawing of Pressurized-Water Loop Equipment.

UNCLASSIFIED
ORNL-LR-DWG 45138

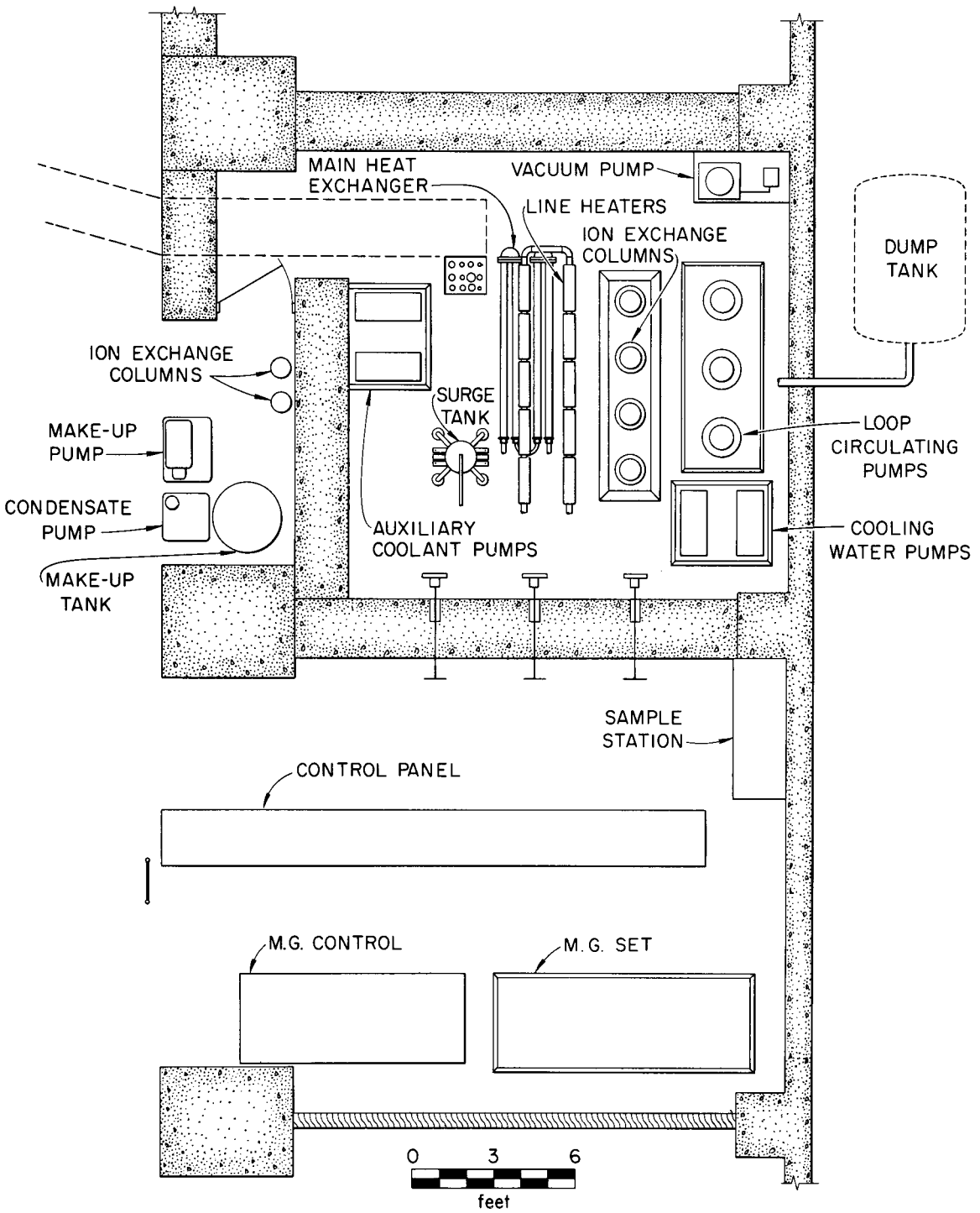

Fig. 3.4. Plan Drawing of Pressurized-Water Loop Equipment.

Fig. 3.5. Operating Area for Pressurized-Water Loop.

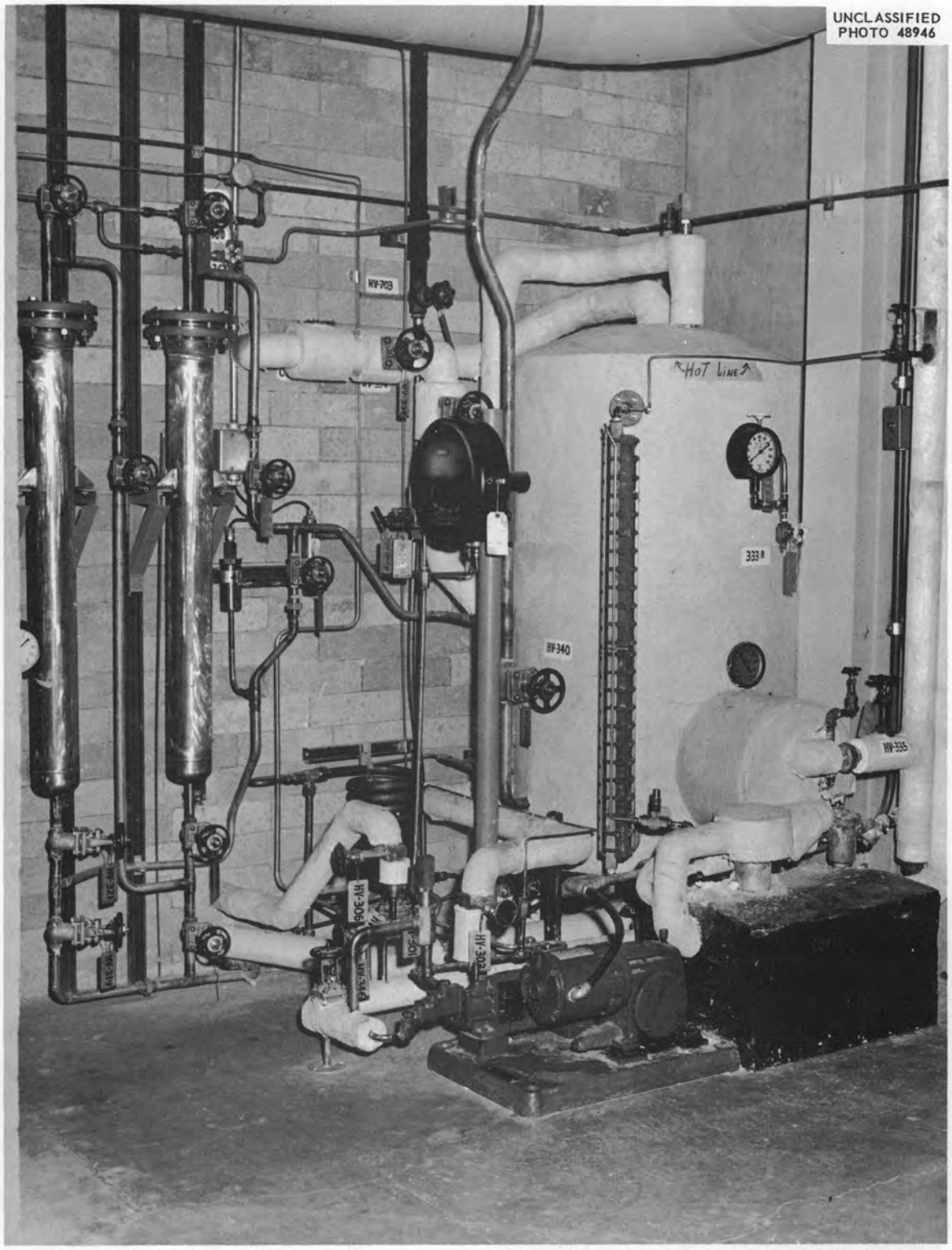

Fig. 3.6. Pressurized-Water Loop Makeup System.

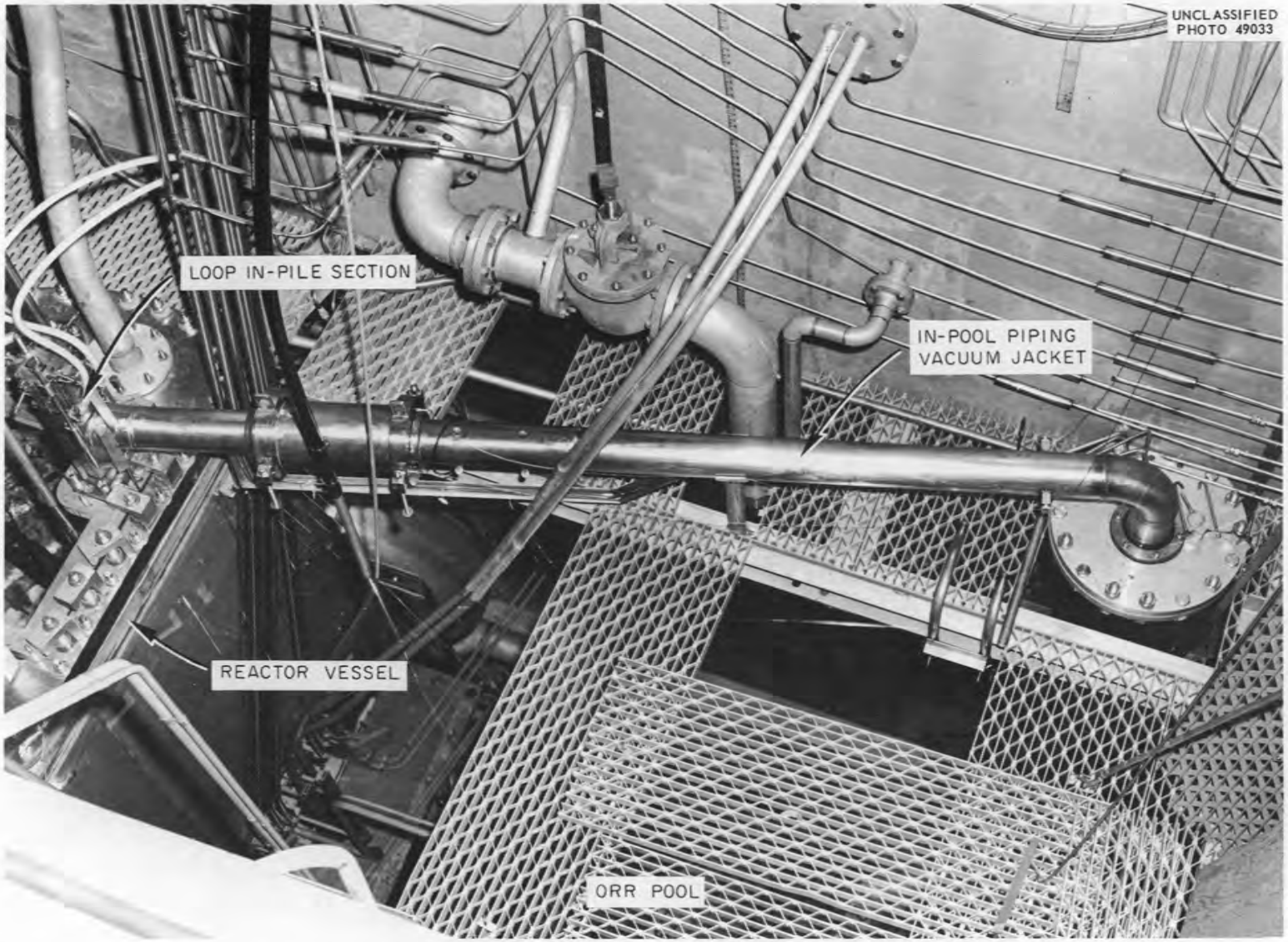

Fig. 3.7. View of ORR Pool Showing Upper End of In-Pile Section of Pressurized-Water Loop and In-Pile Piping Vacuum Jacket.

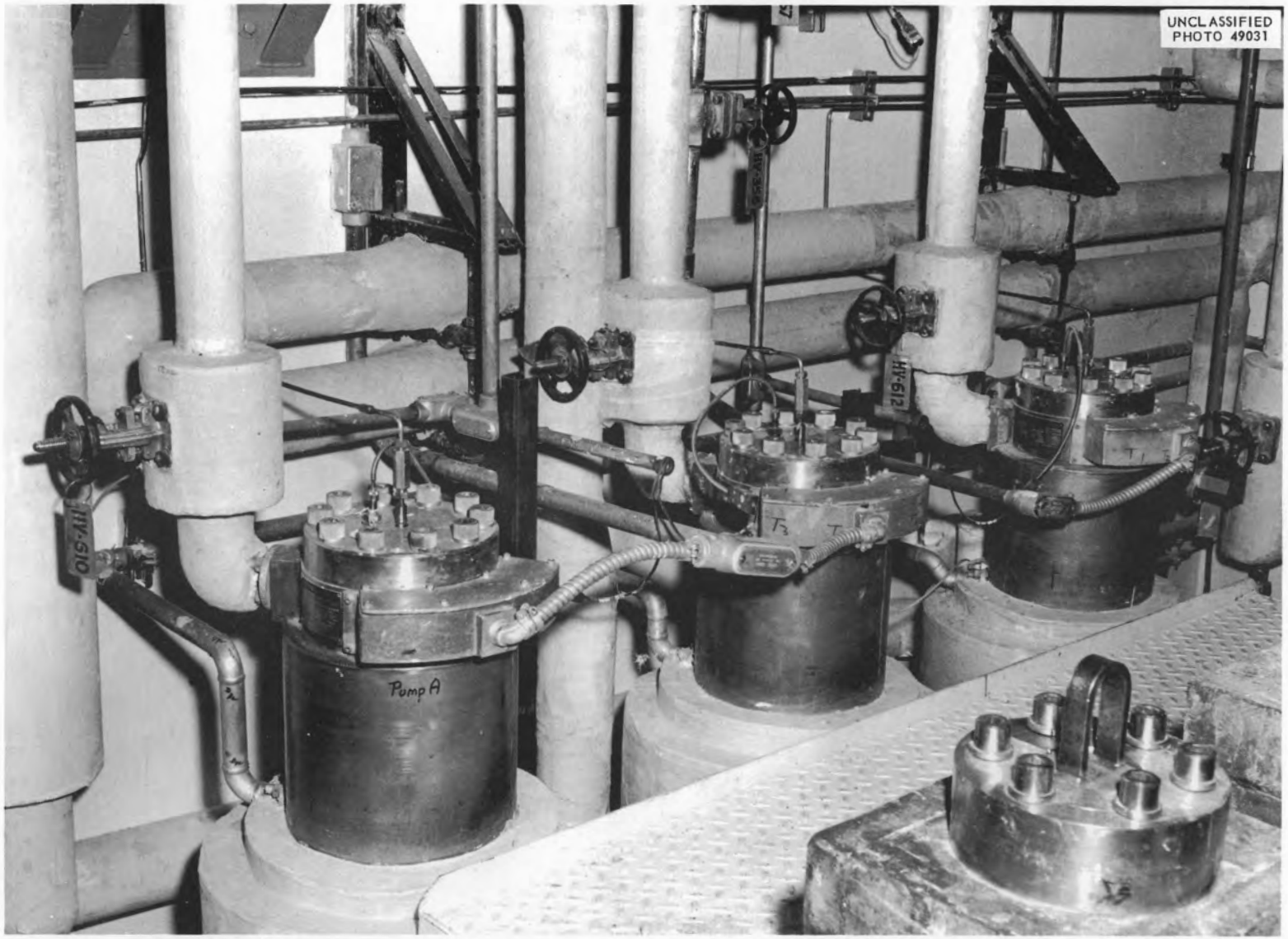

Fig. 3.8. Pumps of Pressurized-Water Loop System.

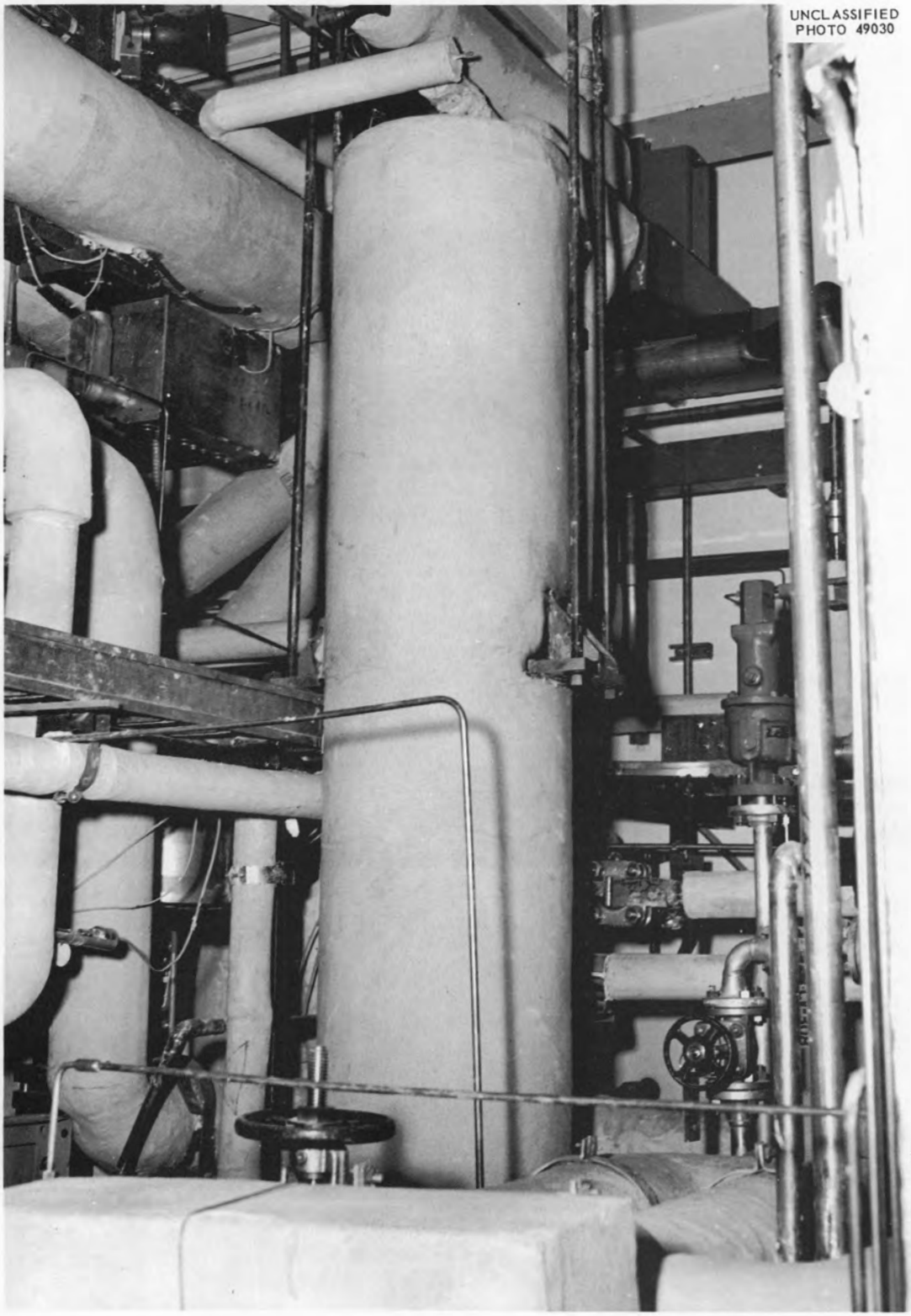

Fig. 3.9. Pressurized-Water Loop Surge Tank.

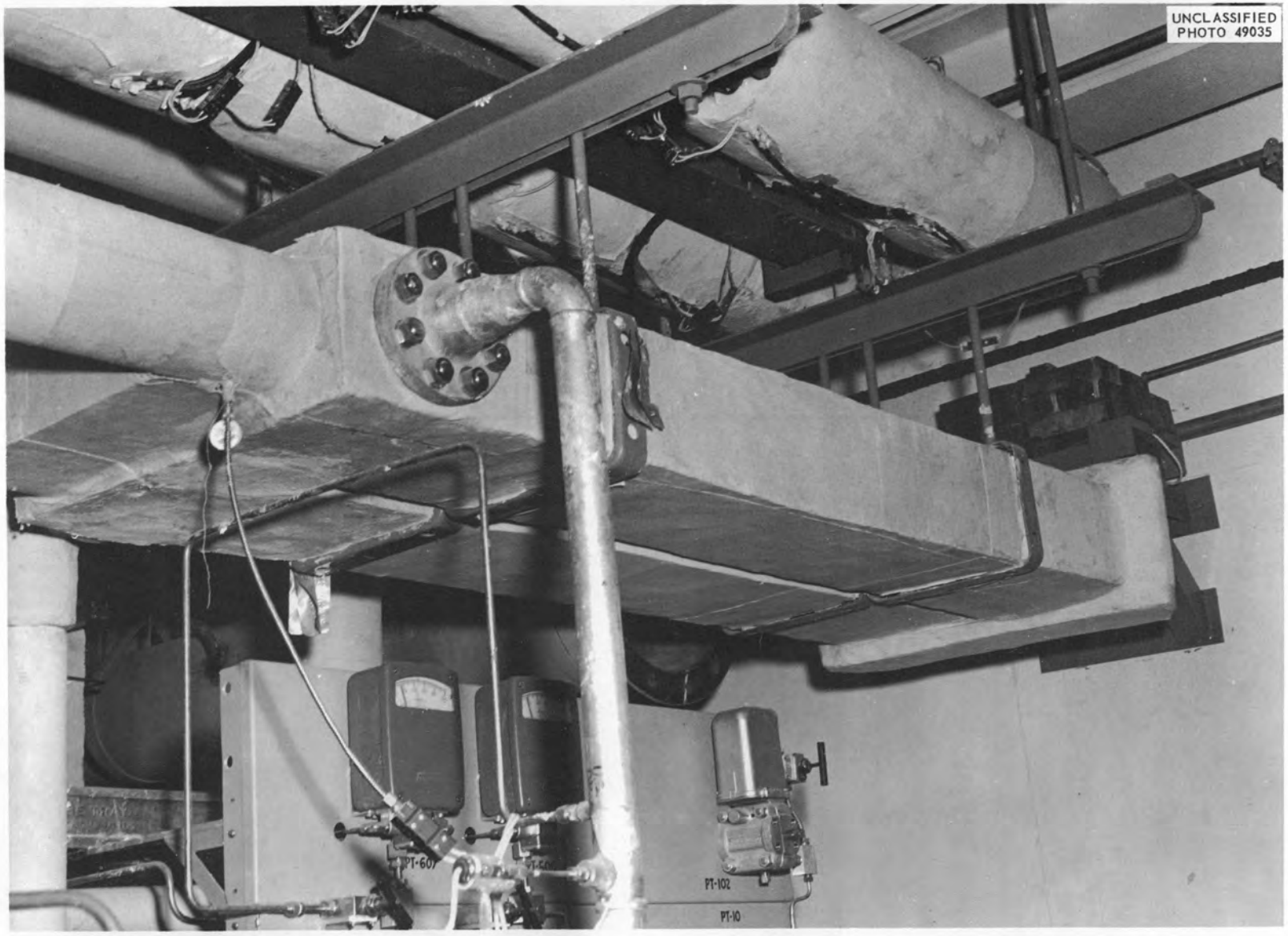

Fig. 3.10. Water-Cooled Heat Exchanger and Line Heaters of Pressurized-Water Loop.

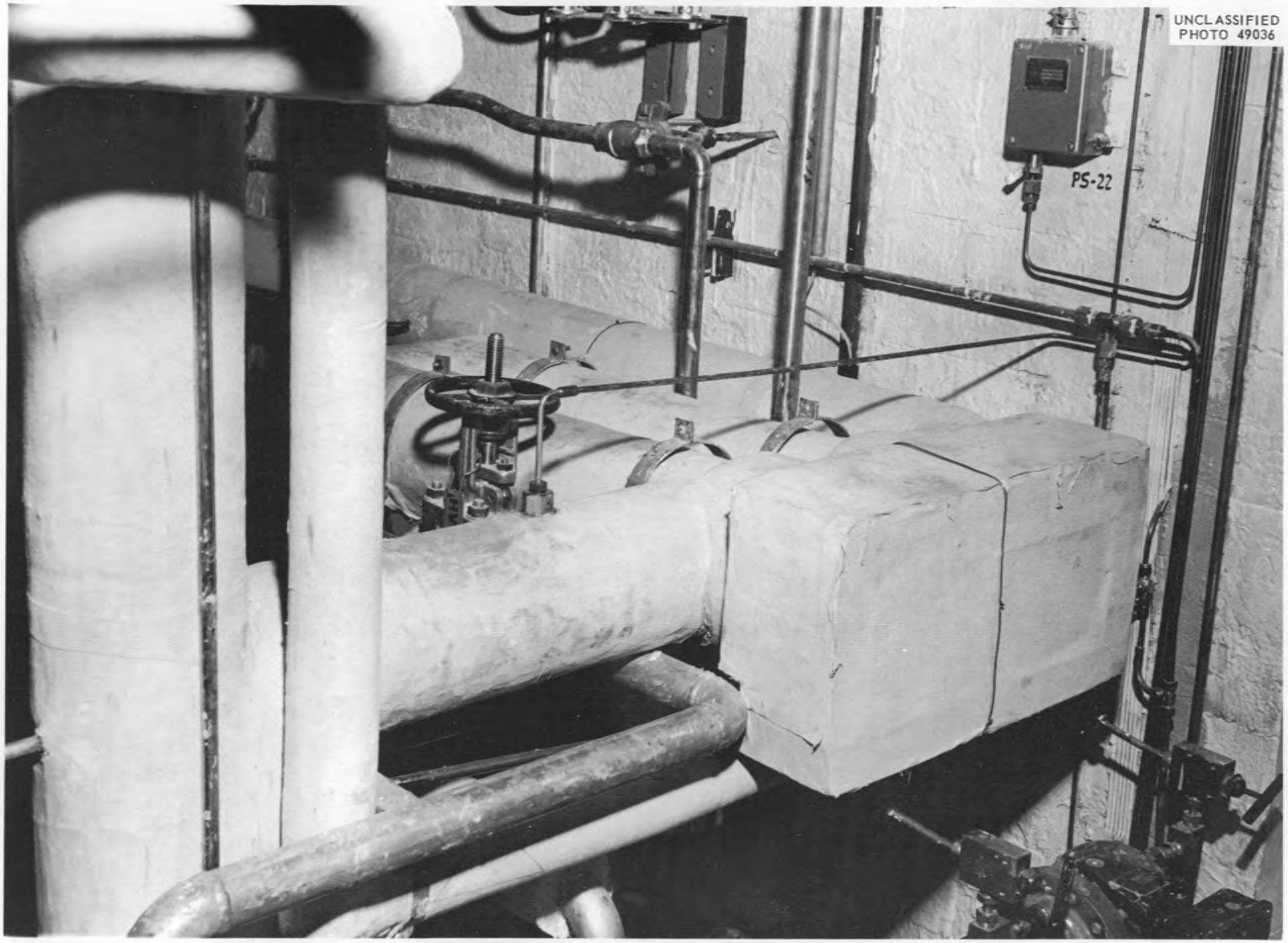

Fig. 3.11. Out-of-Pile Test Section of Pressurized-Water Loop.

Fig. 3.12. Shielded Ion-Exchange Columns and Portion of Transmitter Rack of Pressurized-Water Loop.

Fig. 3.13. Experimental Assembly Used for Fast-Flux Measurements.

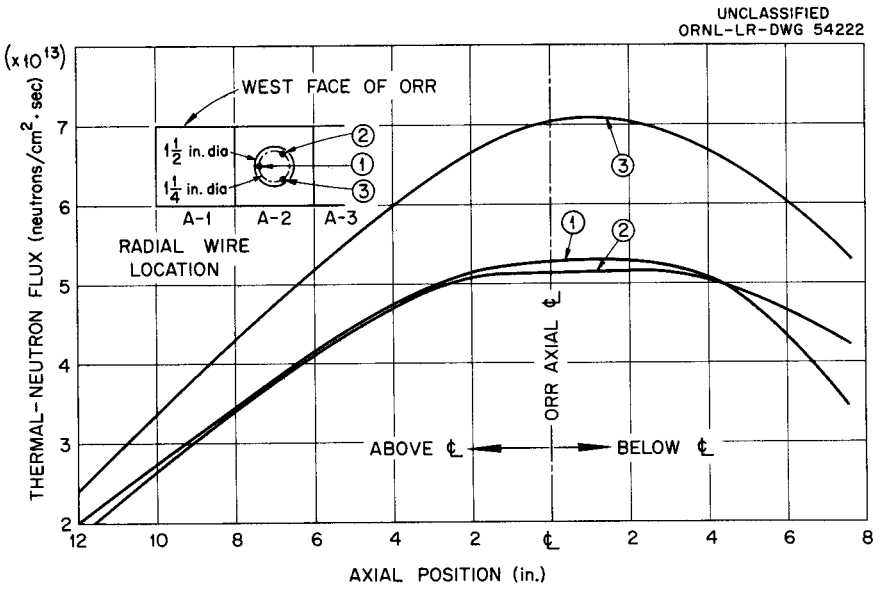

Fig. 3.14. Thermal-Neutron Flux Versus Axial Position in Pressurized-Water Loop Installed in ORR Position A-2 During Reactor Cycle 20 at a Power Level of 20 Mw.

4. ADVANCED CORE DEVELOPMENT

The nuclear core for the N. S. Savannah reactor consists of sintered and pelletized UO_2 fuel bodies contained in type 304 stainless steel fuel tubes. The fuel tubes are assembled into 32 fuel assemblies, and each assembly contains 164 rods. The fuel assemblies are enclosed by stainless steel containers with walls about 0.100 in. thick. The fuel container assembly is a permanent part of the reactor internal structure. It appears that significant improvements relative to fuel fabrication costs and neutron economy can be made in the basic core.

The fuel containers account for about one-third of the total quantity of stainless steel in the core. Also, the containers are located in regions of high neutron flux. For this application, it appears that the usual stainless steel advantages of low fabrication costs and high integrity do not offset the disadvantage of a high nuclear cross section; the permanent nature of the fuel containers and the relatively low operating temperatures are important considerations in arriving at this conclusion. If the stainless steel containers were replaced with containers of a material with a low nuclear cross section, it is expected that a significant improvement in neutron economy and over-all operating costs could be achieved.

The method of UO_2 fuel preparation involves pressing, sintering, grinding, and inspecting individual fuel pellets, of which there are about one-half million in one core loading. It appears that the development of a method of fabricating UO_2 fuel elements utilizing nonsintered fuel would effect a significant reduction in fuel fabrication costs.

The advanced core development effort has been directed toward investigating the feasibility and potential benefits of replacing the present fuel container assembly with a Zircaloy assembly and the development and testing of advanced UO_2 fuel elements. Details of the advanced core work are presented in the following sections.

Zircaloy Fuel-Container Studies

Physics (E. E. Gross)

In a previous report[1] some preliminary results of a comparison of Zircaloy and stainless steel egg-crate structures[2] for the N. S. Savannah core were presented. The analyses indicated that a Zircaloy egg-crate type of core containing 3.1% enriched UO_2 fuel would have about the same cold reactivity as a similar stainless steel core with 4.2% enriched UO_2 fuel. Although the calculated value for the effective multiplication factor for core I of the N. S. Savannah was 1.156, as compared with a measured value[3] of 1.113, the method of analysis was believed to be satisfactory for a comparison of Zircaloy and stainless steel cores of the egg-crate type.

In order to extend the analytical methods to adequately handle control rods and possibly bring the calculated results into better agreement with the measured values, a four-group method was devised. The previous method,[2] although a 24-energy-group method, allowed for inhomogeneous flux distributions only in the thermal-energy group and did not specifically account for the two-dimensional fuel-element arrangement in a full-sized core. The present method accounts for inhomogeneous flux distributions in four energy groups and handles the full-sized core in the geometry of Fig. 4.1. The four-group method gives a calculated value of the effective multiplication factor of 1.110 for core I uniformly enriched 4.2%. This value is in much better agreement with the measured value.

Calculated four-group flux distributions within a fuel pin cell of core I are shown in Fig. 4.2. These results were obtained by using

---

[1] "Maritime Reactor Project Ann. Prog. Rep. Nov. 30, 1959," ORNL-2865, pp. 77–78.

[2] "Comparison of Zircaloy and Stainless Steel as the Structural Materials in the Core of the N. S. Savannah," KT-503 (November 9, 1959).

[3] "Nuclear Merchant Ship Reactor Zero Power Test, Core I," BAW-1202.

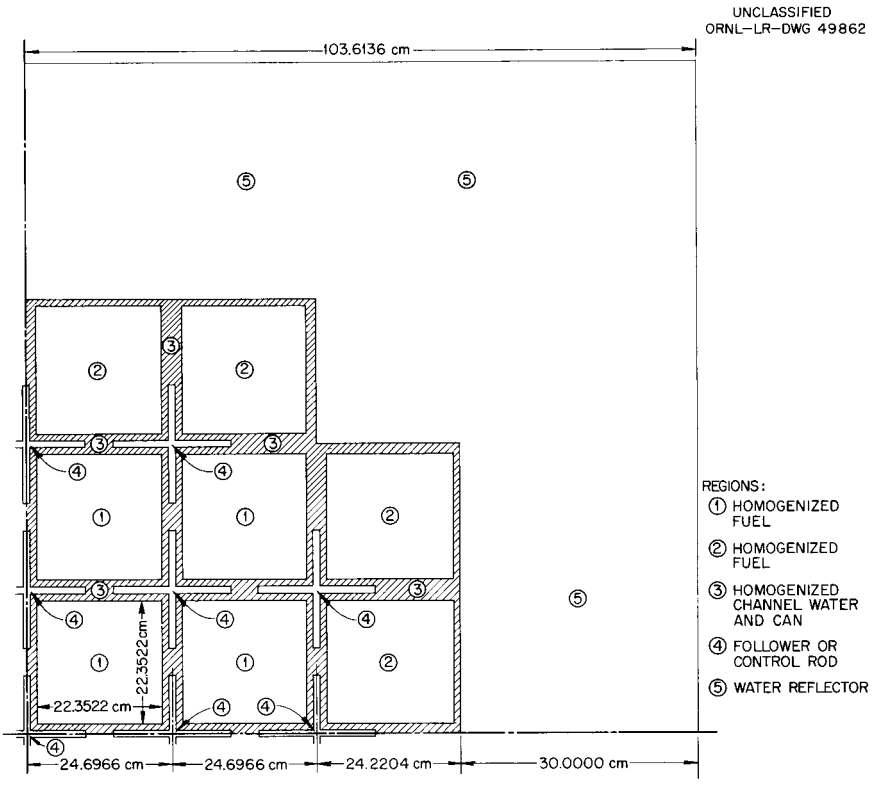

Fig. 4.1. Quadrant of N. S. Savannah Core I.

the S-4 approximations to the S_n method[4] for solving the transport equation. The fuel-pin-cell flux results may be used to obtain four-group cross sections representing a homogenized fuel region.

Four-group, S-5 fluxes throughout a core I fuel element can cell obtained by using the above-mentioned homogenized-fuel-region cross sections are shown in Figs. 4.3 and 4.4. The case with Zircaloy followers present in the water channels between an infinite array of slab fuel cans is presented in Fig. 4.3. The pronounced thermal-flux peaking in the water channel and the perturbing influence of the water channel on the nonthermal fluxes may be seen. The same flux results are shown in Fig. 4.4 for the case with control rods rather than followers present in the water channels between fuel cans. The group-2

[4]B. G. Carlson and G. P. Bell, "Solution of the Transport Equation by the S_n Method," Geneva Conference Paper 2386 (1958).

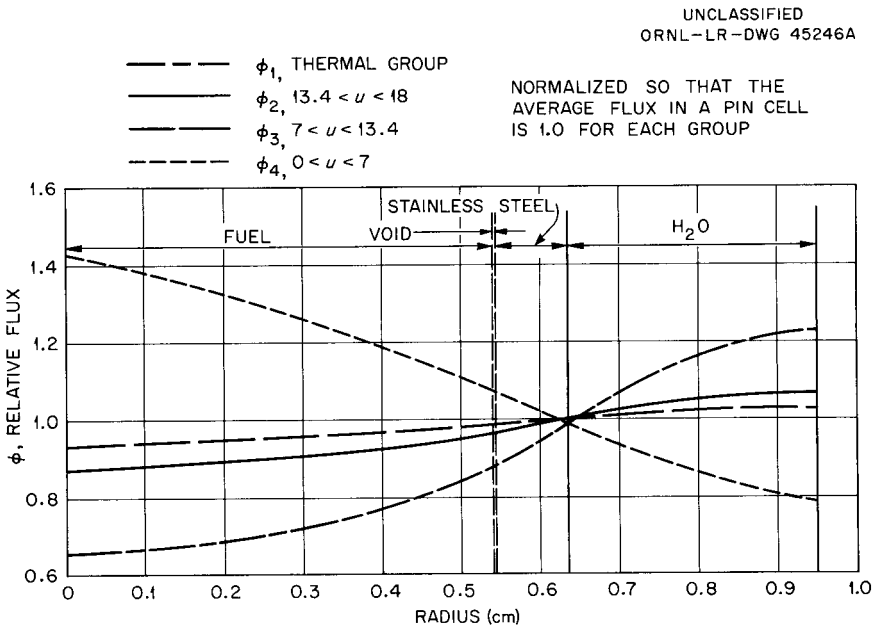

Fig. 4.2. Flux Distributions in N. S. Savannah Core I Pin Cell Based on S-4 Approximation.

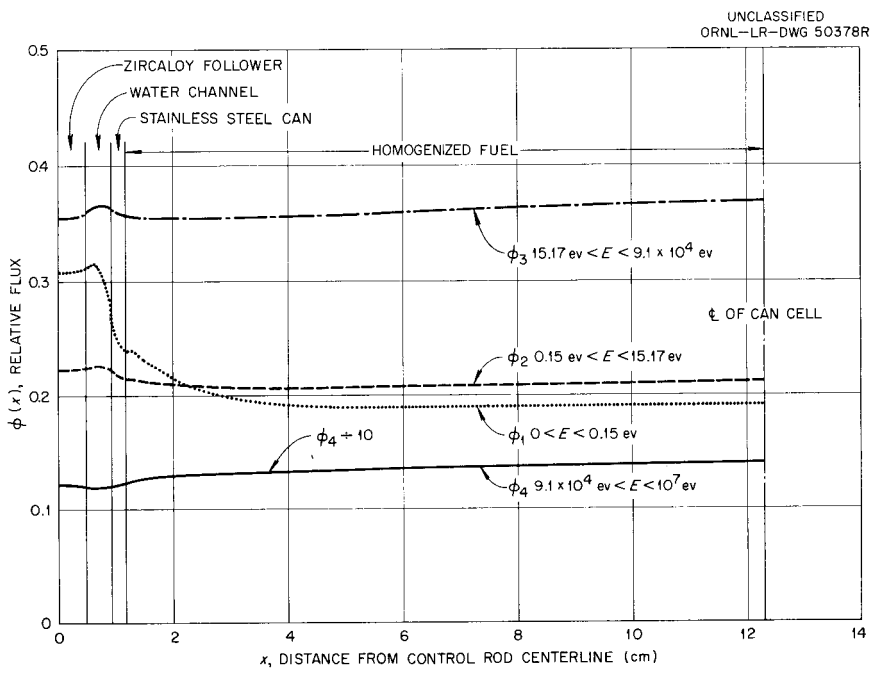

Fig. 4.3. Flux Distributions in N. S. Savannah Core I Control-Rod Follower Can Cell Based on S-5 Approximation.

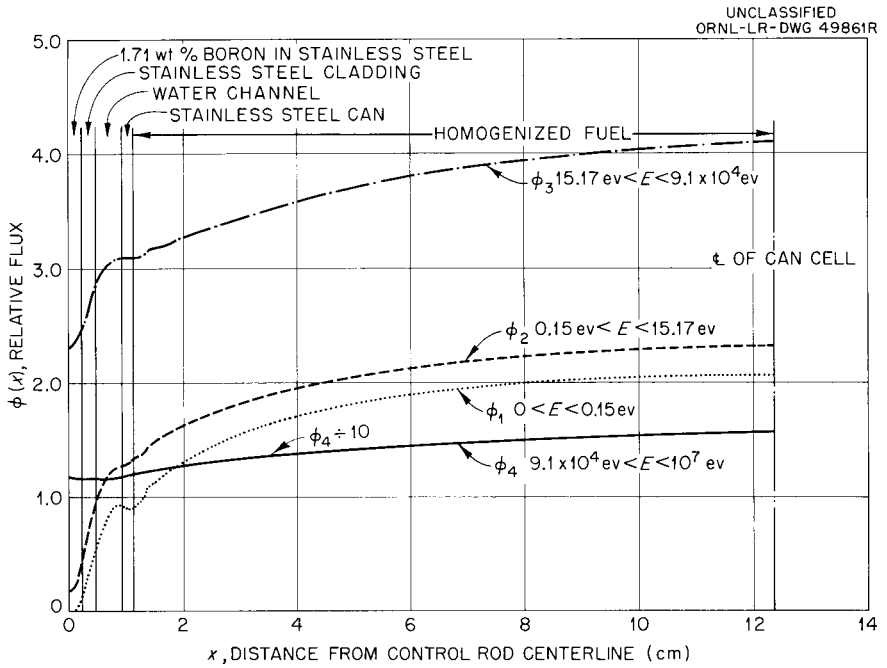

Fig. 4.4. Flux Distributions in N. S. Savannah Core I Control Rod Can Cell Based on S-5 Approximation.

flux distribution (which is the ultimate source of thermal neutrons) may be seen to be far from "flat."

The purpose of the calculation represented in Fig. 4.4 was to provide transport-theory boundary conditions to replace the control rods in a two-dimensional diffusion-theory calculation of the full-sized core. The PDQ code[5] has provisions for a logarithmic-derivative boundary condition in the form of specifying the current per unit flux at the boundary. For a very strong absorber, it is customary to use a "no-return current" or "black body" boundary condition. Diffusion theory gives -0.50 for the current per unit flux at a plane "back boundary" next to a homogeneous diffusing medium, whereas transport theory gives the value -0.47. The values obtained from the results of Fig. 4.4 are

[5]G. G. Bilodeau et al., "PDQ, An IBM-704 Code to Solve the Two-Dimensional Few-Group Neutron Diffusion Equation," WAPD-TM-70 (1957).

shown below:

Group	J/ϕ at Rod Surface
4	−0.0068
3	−0.078
2	−0.325
1	−0.429
"Black body" diffusion theory	−0.5
"Black body" transport theory	−0.47

It may be seen that, although the N. S. Savannah control rods are quite "black" to neutrons in energy group 2, as well as to neutrons in the thermal-energy group, the S-5 values for the current per unit flux at the rod surface are somewhat less than the expected "black body" value of −0.47 for these two groups.

With the use of the control-rod boundary conditions given above and a correction for the difference between a transport-theory calculation and a diffusion-theory calculation using logarithmic-derivative boundary conditions,[6] the calculated control-rod worth in core I uniformly enriched 4.2% is $\Delta k = 0.148$, which compares favorably with the measured value[3] of $\Delta k = 0.133$. Similar calculations on a core using Zircaloy in place of stainless steel for the N. S. Savannah egg-crate core structure indicate that the control-rod worth would be increased by about $\Delta k = 0.05$ by this material substitution. Since the core I reactivity lifetime is based[7] on the excess Δk of 0.047, it would seem that the substitution of Zircaloy for stainless steel in the core I structure offers the attractive possibility of doubling the reactivity lifetime within the same limitation on shutdown margin.

A comparison of power profiles in the stainless steel and Zircaloy cores for the case when only followers are present is presented in

---

[6]B. W. Colston, E. E. Gross, and M. L. Winton, "Heterogeneous Control Rod Studies," Proceedings of the ANPP Reactor Analysis Seminar Held at the Martin Company, Baltimore, Maryland, October 11-12, 1960 (to be published).

[7]"NMSR Final Safeguards Report, Volume I, Description of the N. S. Savannah," p. 36, BAW-1164 (March 1960).

Figs. 4.5 and 4.6. The comparison is on the basis of the same integrated power in both cores. Although the Zircaloy structure produces greater power peaking near the water channels, the gross radial peaking factor is smaller for the Zircaloy core. The net peaking factors appear to be the same for both cores.

An excellent test for any analytical method which attempts to predict the relative properties of N. S. Savannah-type cores containing different structural materials is provided by the Marty II and Marty III critical experiment results.[8] Details of the Marty II critical experiment core are shown in Fig. 4.7. Marty III is identical to Marty II except that the can material is 0.130-in.-thick aluminum rather than 0.156-in.-thick stainless steel. The data[8] obtained in these experiments provide a comparison of the static multiplication factors of Marty II and Marty III for various control rod configurations in a 16-can core. These

[8]"NMSR Project Quarterly Technical Report, April-June 1958," BAW-1118, pp. 75–80.

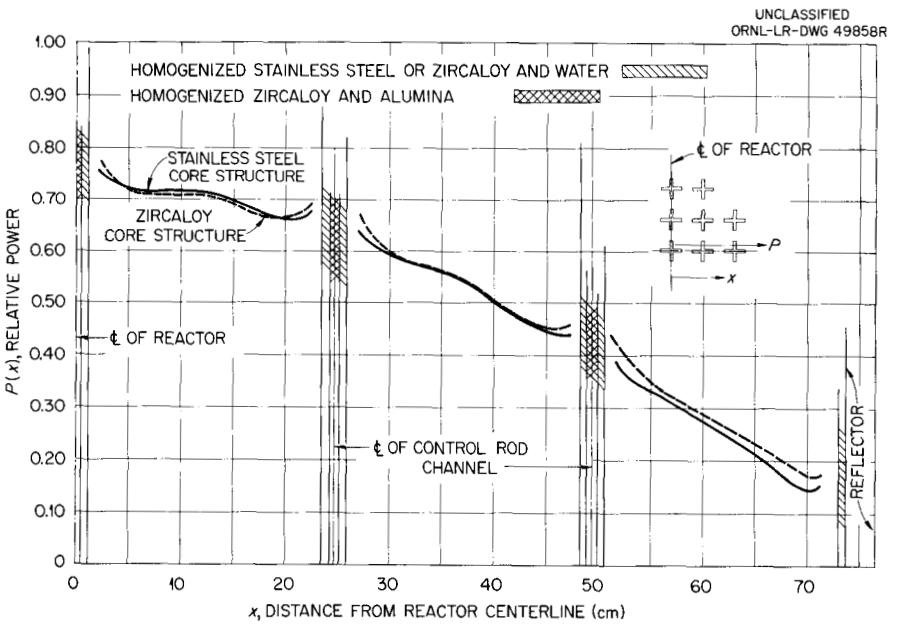

Fig. 4.5. Comparison of Horizontal Power Distributions for N. S. Savannah Stainless Steel and Zircaloy Core Structures.

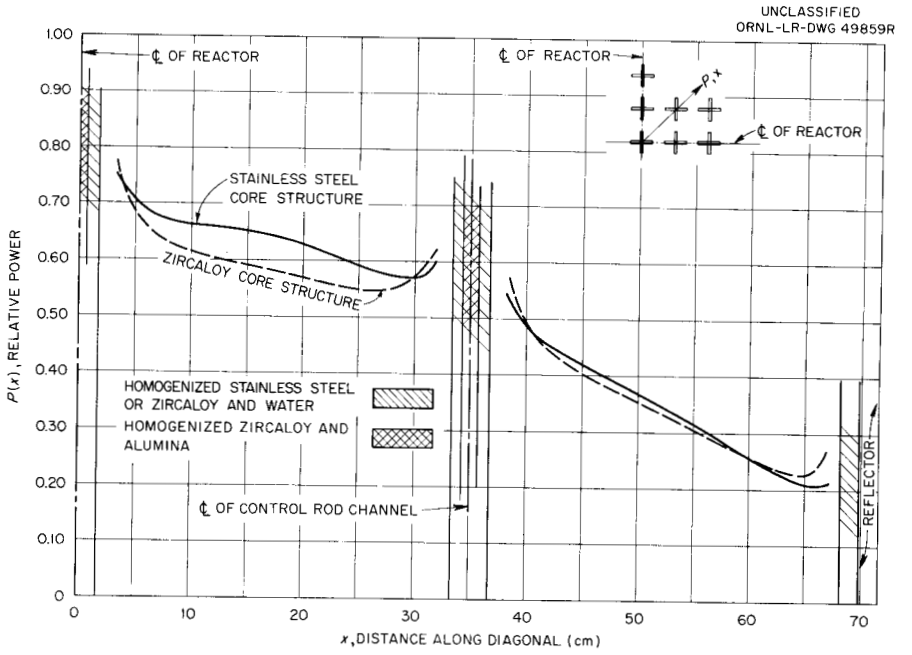

Fig. 4.6. Comparison of Diagonal Power Distributions for N. S. Savannah Stainless Steel and Zircaloy Core Structures.

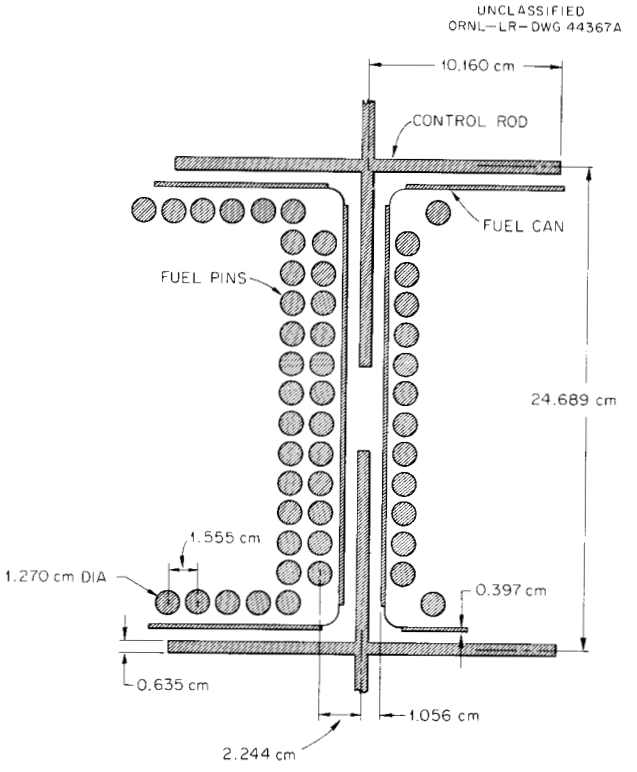

Fig. 4.7. Portion of Marty II Critical Experiment Core.

experimental cores did not contain followers, and a retracted control rod was therefore replaced by water.

The geometry used to represent these experimental cores is shown in Fig. 4.8. It should be noted that the missing corner pins (see Fig. 4.7) are accounted for by extending the water region into the fuel pin region. A comparison of experimental and analytical results is presented in Fig. 4.9. The indicated experimental errors are based only on reproducibility of critical water-height positions. Considering the uncertainties in the cross-section information and the inhomogeneous nature of the core, it is perhaps fortuitous that the experimental and calculated static multiplication factors agree so closely. Of particular note, however, is the success of the calculational method in reproducing the effect of the structural material on control-rod worth.

Zircaloy Properties (C. L. Whitmarsh)

A search of the available literature relative to the technology of Zircaloy-2 and Zircaloy-4 was made with respect to the possible use of Zircaloy as a material of construction in an advanced core for the N. S. Savannah. The available information has not been completely analyzed, but, based on present information, either Zircaloy-2 or Zircaloy-4 appears to be a satisfactory material for the fuel-element container. Experience with Zircaloy-4 under reactor service conditions is at present limited; but it has been demonstrated in experiments that Zircaloy-4 has less tendency to pick up hydrogen, with resulting embrittlement of the metal. This is an advantage over Zircaloy-2, since hydrogen pickup may be the limiting condition for long-term reactor service in the N. S. Savannah. Although 20-year service-life predictions necessitate extrapolation of creep, corrosion, and irradiation data by factors of 10 to 15, existing data do not indicate any insurmountable problems. Additional data will become available from in-reactor service and from considerable experimental work being performed at various sites.

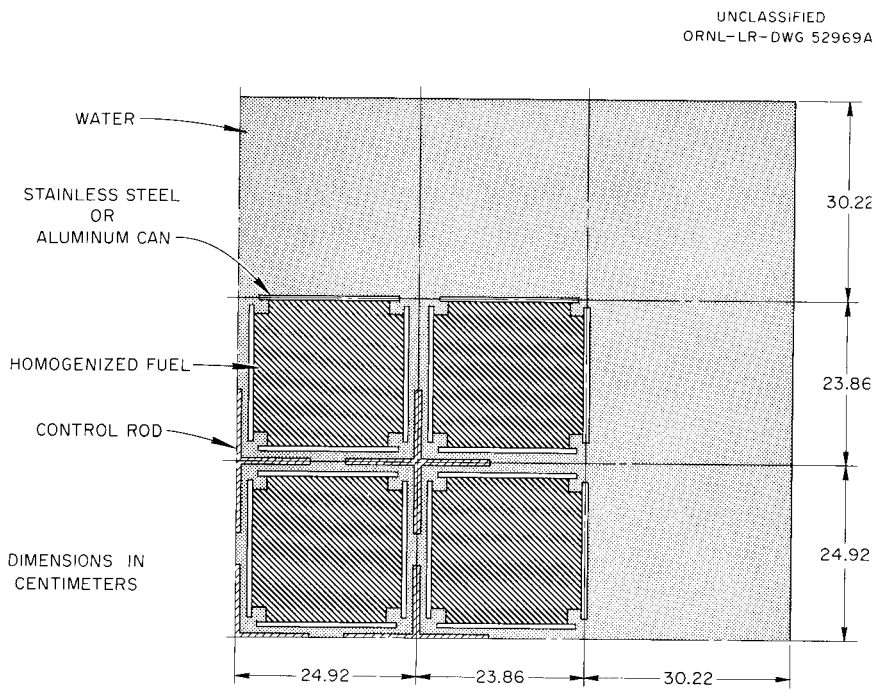

Fig. 4.8. Quadrant of 16-Can Marty II or Marty III Critical Experiment Core.

UNCLASSIFIED
ORNL-LR-DWG 52970

ROD PATTERN	MARTY II		MARTY III	
	K_s EXP	K_s CALC	K_s EXP	K_s CALC
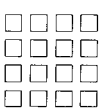	1.047 ± 0.001	1.048	1.17 ± 0.02	1.173
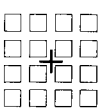	1.026 ± 0.001	1.024	1.14 ± 0.02	1.141
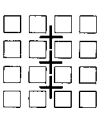	1.0007 ± 0.0001	0.994	1.10 ± 0.02	1.092
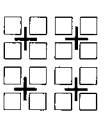	1.013 ± 0.001	1.015	1.12 ± 0.02	1.119

Fig. 4.9. Comparison of Calculated and Experimental Static Multiplication Factors in Marty II and Marty III Critical Experiments.

Fuel Development

Rotary Swaging of Stainless Steel-Clad UO_2 Fuel Rods (R. J. Beaver, J. T. Lamartine, W. C. Thurber)

Techniques are being studied for producing stainless steel-clad high-density UO_2 fuel rods of superior integrity by rotary swaging of loose UO_2 powder in capped stainless steel tubes. Efforts have been made to evaluate the swageability of commercially produced swageable UO_2, to determine the effects of swaging reduction and temperature on wall cracking in the stainless steel cladding of swaged rods, and to prepare swaged UO_2 fuel capsules for irradiation in the pressurized-water loop in the Oak Ridge Research Reactor (ORR).

Comparison of Commercially Produced Swageable Grades of UO_2. Since swaged UO_2 fuel rods are being seriously considered for future cores of the N. S. Savannah reactor, a study has been conducted to investigate the swaging characteristics of commercially produced swageable UO_2. The three types of UO_2 which have been evaluated are described in Table 4.1. Each type of UO_2 was packed by hand in a 0.750-in.-o.d., 0.035-in.-wall, type 304 stainless steel tube and reduced 55% in area by swaging at temperatures ranging up to 900°C. The effect of the swaging temperature on the density of the UO_2 is shown in Fig. 4.10. Each data point is the average of the data of several experiments. Maximum density was achieved at 800°C with both the high-fired type A oxide and the fused-and-ground

Table 4.1. Properties of Commercially Available UO_2 Examined for Swageability in Stainless Steel Tubes

Oxide Identification	General Type	Tapped Bulk Density (g/cm^3)	Surface Area (m^2/g)	Oxygen-to-Uranium Ratio	Particle Size Distribution (mesh)
A	High fired	5.89	0.07	2.012	-80 +100 (9.3%), -100 +170 (21.7%), -170 +325 (31.0%), -325 (38.0%)
B	Fused and ground	6.45	0.05	2.026	-20 +32 (15.1%), -32 +65 (35.0%), -65 +80 (5.3%), -80 +100 (7.6%), -100 +170 (10.9%), -170 +325 (12.3%), -325 (13.8%)
C	High fired	5.00	0.02	2.041	-100 +170 (12.0%), -170 +325 (61.6%), -325 (26.4%)

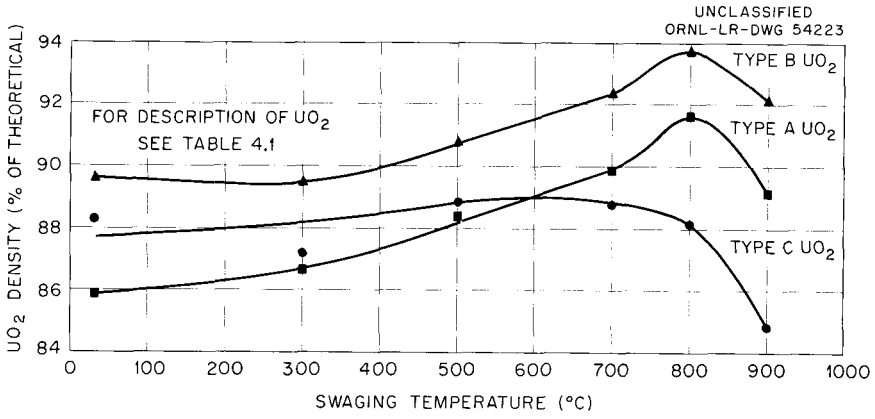

Fig. 4.10. Effect of Swaging Temperature on Density of Three Commercially Produced Swageable Grades of UO_2 at Constant Reduction in Area of 55%.

type B oxide. The higher maximum density of 93.8% for the fused-and-ground oxide compared with the 91.7% value for type A high-fired oxide is attributed principally to the higher tapped bulk density and larger particle size of the fused-and-ground oxide.

The high-fired type C oxide exhibited anomalous behavior compared with the type A high-fired oxide. Although its density after swaging at room temperature was higher than that of the type A oxide, its density decreased at temperatures above 600°C, whereas, the density of the type A oxide continued to increase to a maximum at 800°C. The reason for this behavior has not been determined.

Effects of Swaging Temperature and Reduction on Wall Cracking of Cladding. One of the problems encountered in the swaging of UO_2 fuel rods was the appearance of cracks in the stainless steel cladding, particularly in rods swaged at elevated temperatures. A typical crack is illustrated in Fig. 4.11. An investigation was therefore conducted to determine the interrelationship between swaging temperature and total swaging reduction on the tendency of the type 304 stainless steel cladding to crack. The results of this study, presented in Fig. 4.12, indicate that with cold reductions in area of less than 65% and swaging temperatures of less than 600°C, crack-free cladding is obtained. Outside these boundary conditions, cracks of various magnitudes are likely to occur

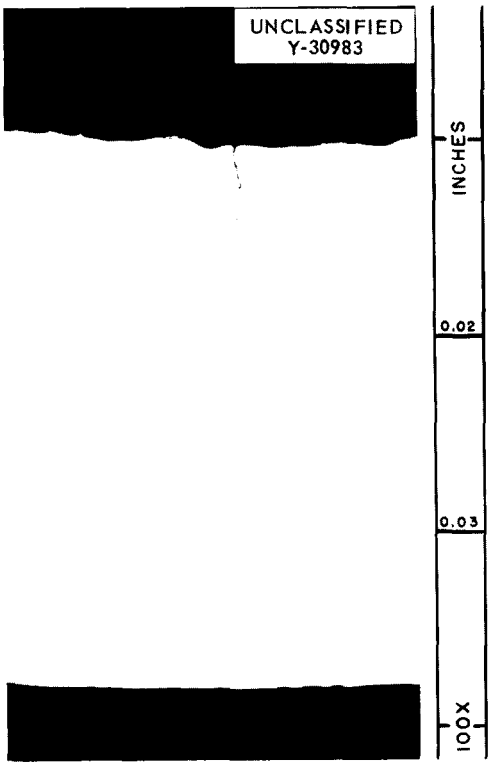

Fig. 4.11. Photomicrograph of Swaged Type 304 Stainless Steel Tubing Showing a Typical Wall Crack. As polished. 100X.

Preparation of Swaged-UO_2, Stainless Steel-Clad, Irradiation-Test Specimens. An irradiation testing program is being conducted in the pressurized-water loop in the ORR for evaluating the performance of stainless steel-clad swaged-UO_2 fuel rods. The test specimens, shown previously,[9] are triaxial arrays of 18-in.-long, 1/2-in.-diam rods containing fused-and-ground UO_2 of approximately 90% density clad with 0.035-in.-wall, type 304L stainless steel. The rods are spaced at two points along the axial center of the array with ferrule spacers brazed into place with preplated electroless nickel brazing alloy. The perforated fixtures, which are welded to each end of the test element, position the array in the loop.

Four test bundles have been fabricated, two for each of two irradiation tests. One bundle in each experiment consists of three rods swaged at room temperature. The other bundle contains one rod swaged at room temperature and two rods swaged at 800°C. The effect of central fuel temperatures ranging from approximately 2000 to 2500°C on fission-gas release from both room-temperature and 800°C-swaged UO_2 will be evaluated. Effect of initial UO_2 particle size will also be examined.

---

[9]"Maritime Reactor Project Ann. Prog. Rep. Nov. 30, 1959," ORNL-2865, p. 63, Fig. 4.18.

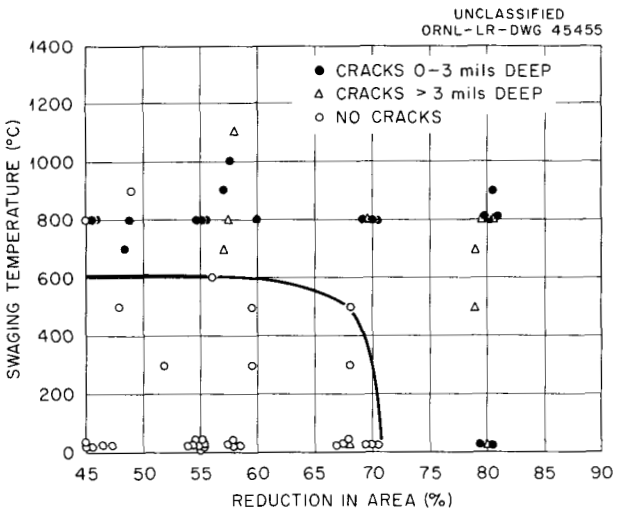

Fig. 4.12. Effect of Swaging Temperature and Reduction in Area on Wall Cracking of Type 304 Stainless Steel Tubing Containing UO_2.

Fabrication of Fuel Rods by Vibratory Compaction (W. Ernst, W. O. Harms, W. C. Thurber)

A program has recently been initiated in which vibratory compaction of bulk UO_2 is being examined as a technique for fabricating fuel rods of the type used in core I of the N. S. Savannah. This method of fabrication appears to offer several advantages over rotary swaging for producing rods containing nonsintered UO_2, including (1) elimination of tube wall cracking, (2) simplification of inspection, and (3) adaptability to remote operation. Both vibratory compaction and swaging appear to be more economical than pelletizing for producing fuel rods.

During the past year the vibratory compaction process has been under study at ORNL as part of a fuel cycle program in which ThO_2–5% UO_2 is the reference fuel. Results obtained from this program have indicated that fused-and-ground oxides can be compacted to approximately 89% of theoretical density using simple low-cost pneumatic equipment. These studies have also demonstrated that multiple-tube bundles can be simultaneously compacted. Present plans call for extension of these studies to fuels and fuel-rod geometries of interest to the Maritime program.

In addition to studies with pneumatic vibrators, some tests were made for ORNL at the Savannah River Laboratories with an electronic device. Malfunctioning of the electronic amplifier which drives the shaker occurred during the tests, and no valid data were obtained. This experiment will be repeated when the equipment is repaired. Irradiation experiments on vibration-compacted fuel in both the VBWR and the pressurized-water loop at the ORR are planned for the near future.

Development of Compartmented Fuel Plates (R. G. Gilliland, G. M. Slaughter, W. C. Thurber)

Compartmented-plate fuel elements in which platelets of a ceramic fuel (e.g., UO_2) are enclosed within a compartmented frame between cover sheets have several advantages over the more conventional tube-bundle design presently employed in most pressurized-water reactors.[10] Among these advantages are greater heat-transfer area, lower central temperatures (with less fission-gas release), the possibility of operating at higher specific power without central melting, less self-shielding of fuel, and less fission-product release from a single cladding defect.

The developmental work presently being conducted on compartmented fuel plates involves the investigation of methods for fabricating stainless steel fuel elements containing several individual leaktight compartments. One method of fabrication which has been studied extensively is based on the formed and spot-welded strip design described previously.[11] Using this design and a special spot-welding fixture, a type 304 stainless steel test-dummy fuel plate was assembled and brazed using preplated electroless nickel as the brazing alloy.[12] Evaluation of this test element revealed numerous areas of nonbonding and resultant intercompartmental leakage. In addition, several brazed joints ruptured during pressurizing tests because of the unbonded areas. A sketch of the apparatus used to pressurize individual compartments is shown in Fig. 4.13. The unbonded areas in the brazed joints are thought to have resulted from a tilting of the formed strips during the assembly operation and the consequent gap being too wide to be bridged by the brazing alloy.

The failure of the formed and spot-welded strip design to produce satisfactory plates prompted the consideration of two other designs. One of these is a compartmented fuel plate which contains grids integral

---

[10]W. C. Thurber, "Some Design Considerations in Compartmented Plate-Type Fuel Elements Containing UO_2," ORNL CF-58-7-105 (July 28, 1958).

[11]"Maritime Reactor Project Ann. Prog. Rep. Nov. 30, 1959," ORNL-2865, pp. 50–54.

[12]P. Patriarca et al., "Electroless-Plated Brazing Alloy," ORNL-2243 (March 19, 1957).

with the frame. The "Elox," or electrical discharge machining method, makes possible the fabrication of this type of frame and grid, shown in Fig. 4.14. The other design incorporates a machined frame whose compartments are transverse to the long axis of the frame. Strips positioned

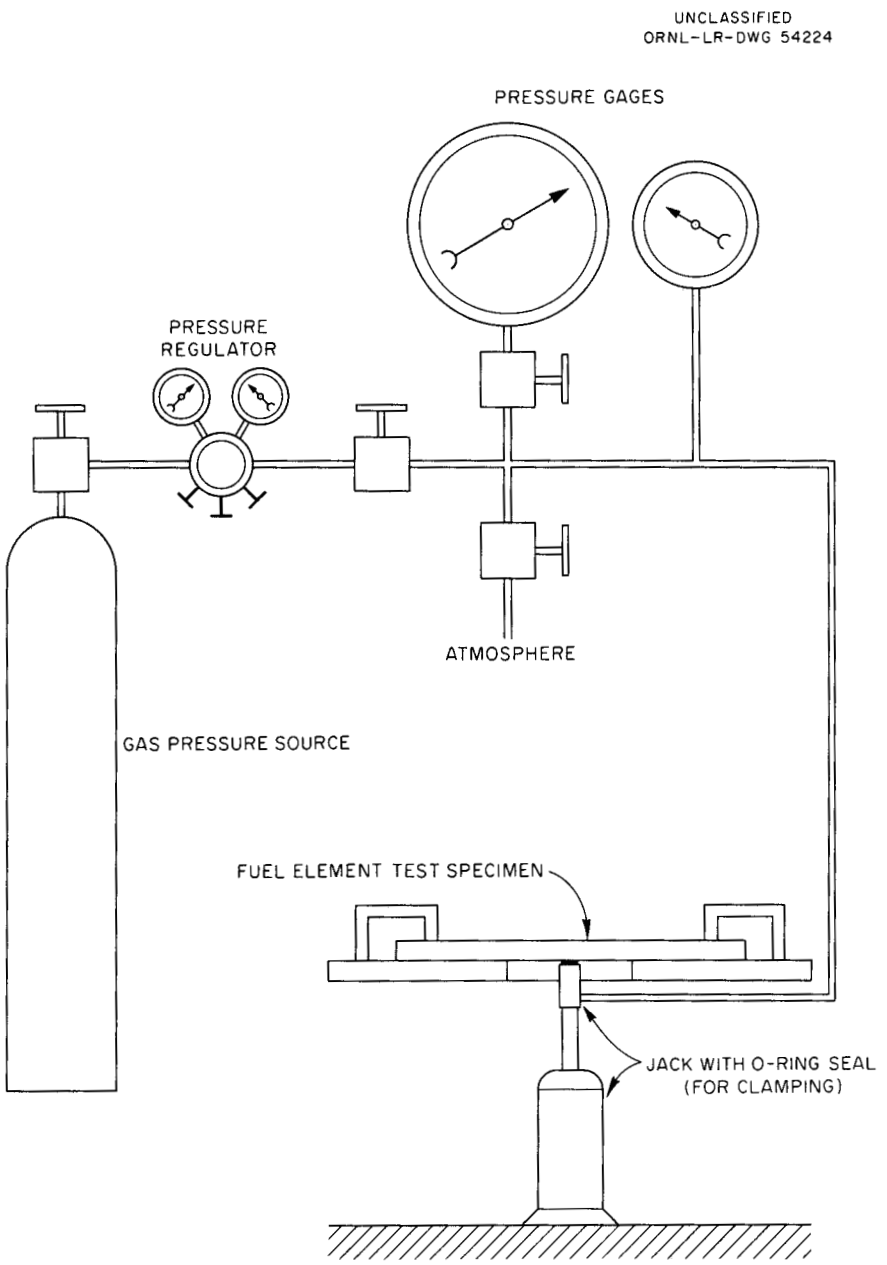

Fig. 4.13. Apparatus for Room-Temperature Pressurizing Tests on Compartmented Fuel Plates.

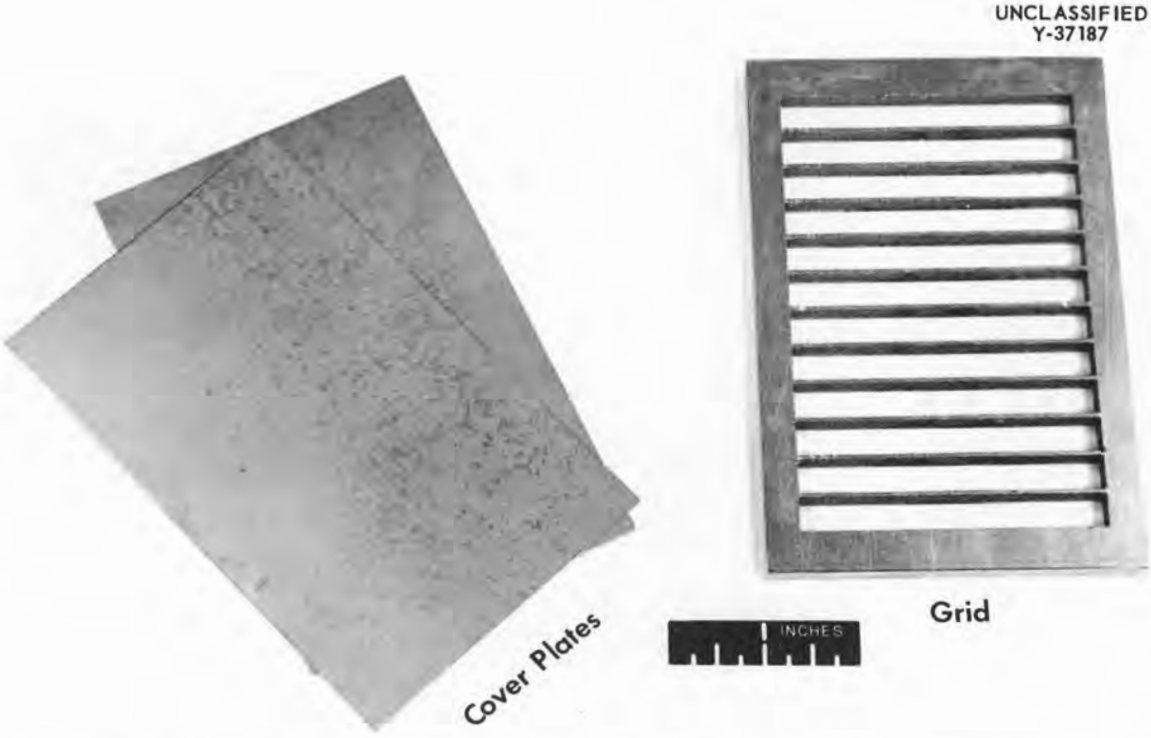

Fig. 4.14. Components of Elox-Machined Compartmented Fuel Element.

during assembly form the fuel receptacles, as shown in Fig. 4.15. These designs should minimize the brazing gap present in the spot-welded strip design and make attainment of individual leaktight compartments a more realistic objective. The evaluation of these new designs is currently in progress.

Another method of bonding cover sheets to the grids of compartmented fuel elements utilizes resistance welding instead of brazing. This is being studied on a subcontract at Sciaky Brothers, Inc., of Chicago, Illinois. Phase I of this subcontract work was concerned with the applicability of resistance welding to the general fuel element fabrication problems and more specifically the feasibility of joining thin sections (cover sheets) to thick sections (frames). The results of the phase I work indicated that it was possible to produce satisfactory joints. The structures of the resistance welds in the transverse and longitudinal directions, are shown in Figs. 4.16 and 4.17, respectively.

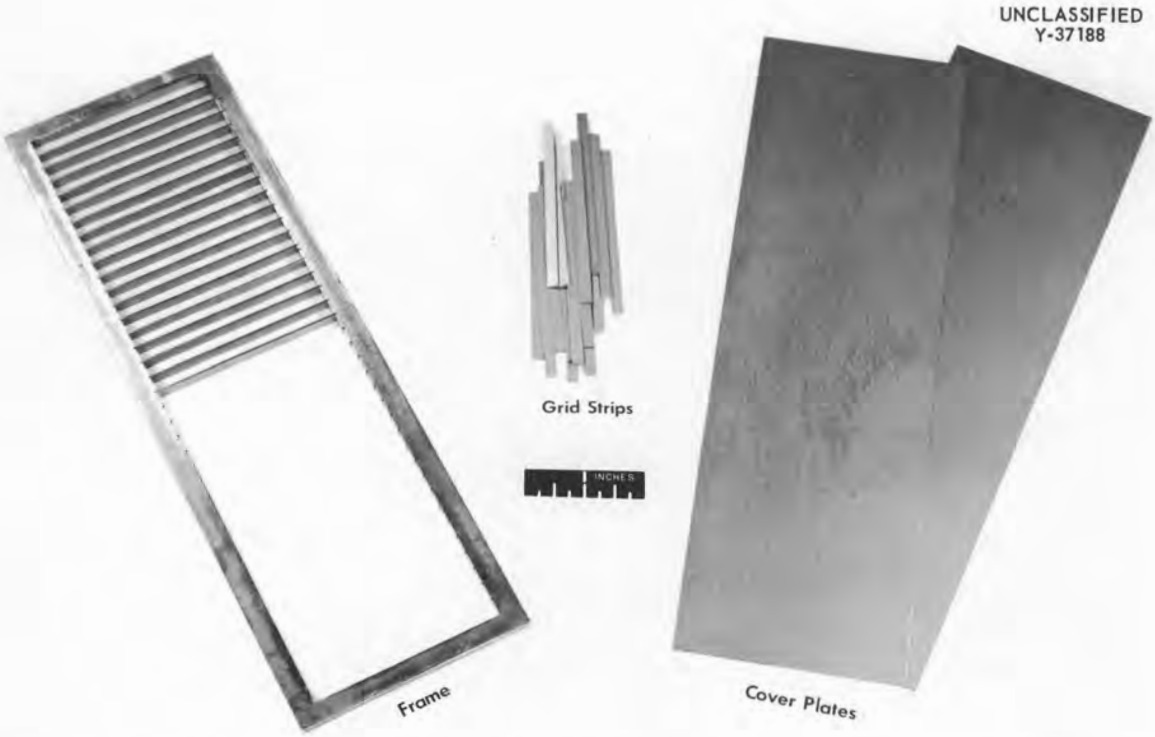

Fig. 4.15. Components of Transverse Strip Compartmented Fuel Element.

The joints shown were produced on type 304L stainless steel using a 0.016-in.-thick cover sheet and a solid 0.190-in.-thick frame.

The resistance-welding subcontract work is currently in phase II, which is concerned with the application of the process to the actual compartmented fuel element containing a grid. The utilization of this process on the formed and spot-welded strip-grid design yielded unsatisfactory results. As in the case of brazing, the tilting of the strip-grid members caused overheating of the thin rib and inconsistent bonding resulted. Currently, studies are in progress to investigate the application of the resistance-welding process to the new "Elox"-machined compartmented fuel element design.

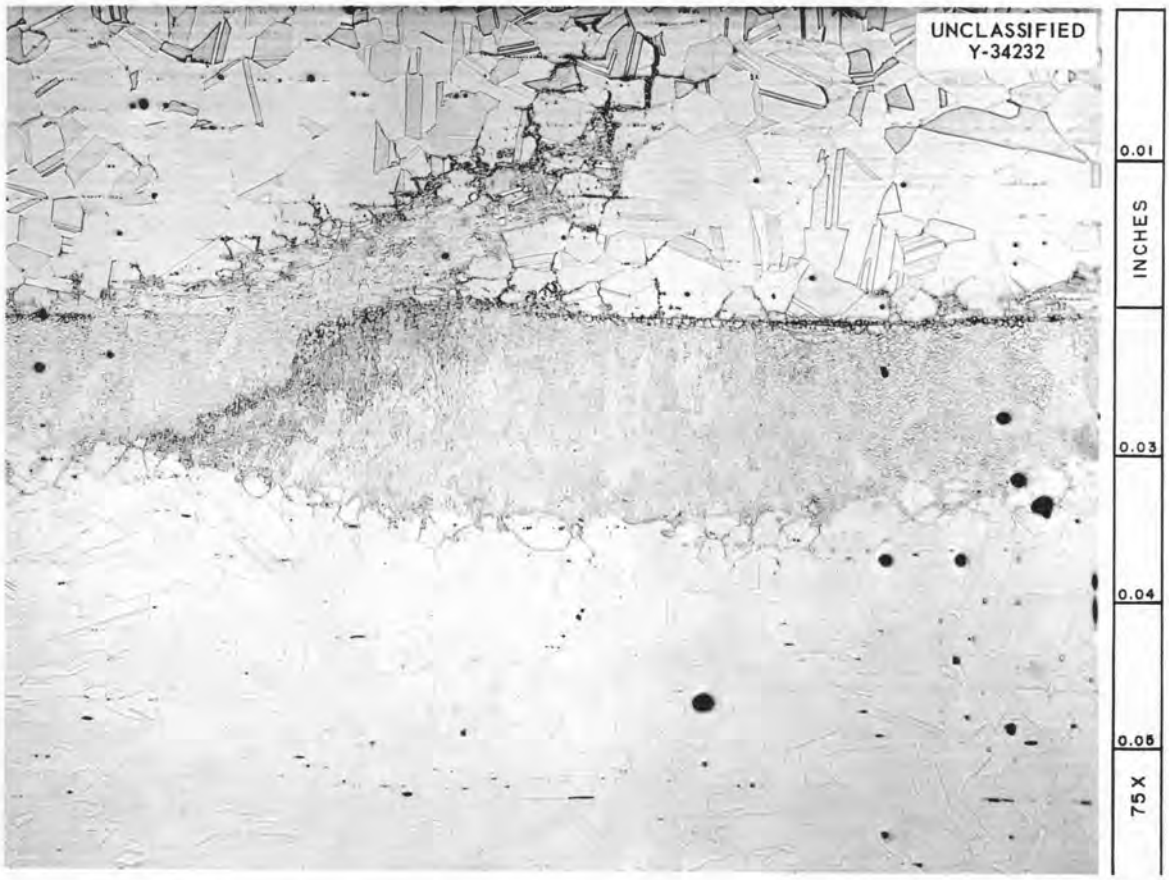

Fig. 4.16. Longitudinal Section of Spot Weld Between a 0.016-in.-Thick Type 304L Stainless Steel Cover Sheet and a 0.190-in.-Thick Type 304L Stainless Steel Frame Showing Character of Bond at Two Overlapping Welds. Etchant: 5% CrO_3-electrolytic.

Irradiation Tests

(V. O. Haynes, W. C. Thurber)

Twelve swaged UO_2 fuel rods arranged in three-rod clusters have received various amounts of irradiation in the pressurized-water loop in the ORR. The effects of irradiation on the behavior of the swaged UO_2 fuel with respect to UO_2 particle size, hot or cold swaging, heat generation rate, and burnup are to be investigated in postirradiation examinations. Two of these clusters, identified as experiment 1, have received irradiation during one 20-Mw, one 16-Mw, and one 30-Mw ORR

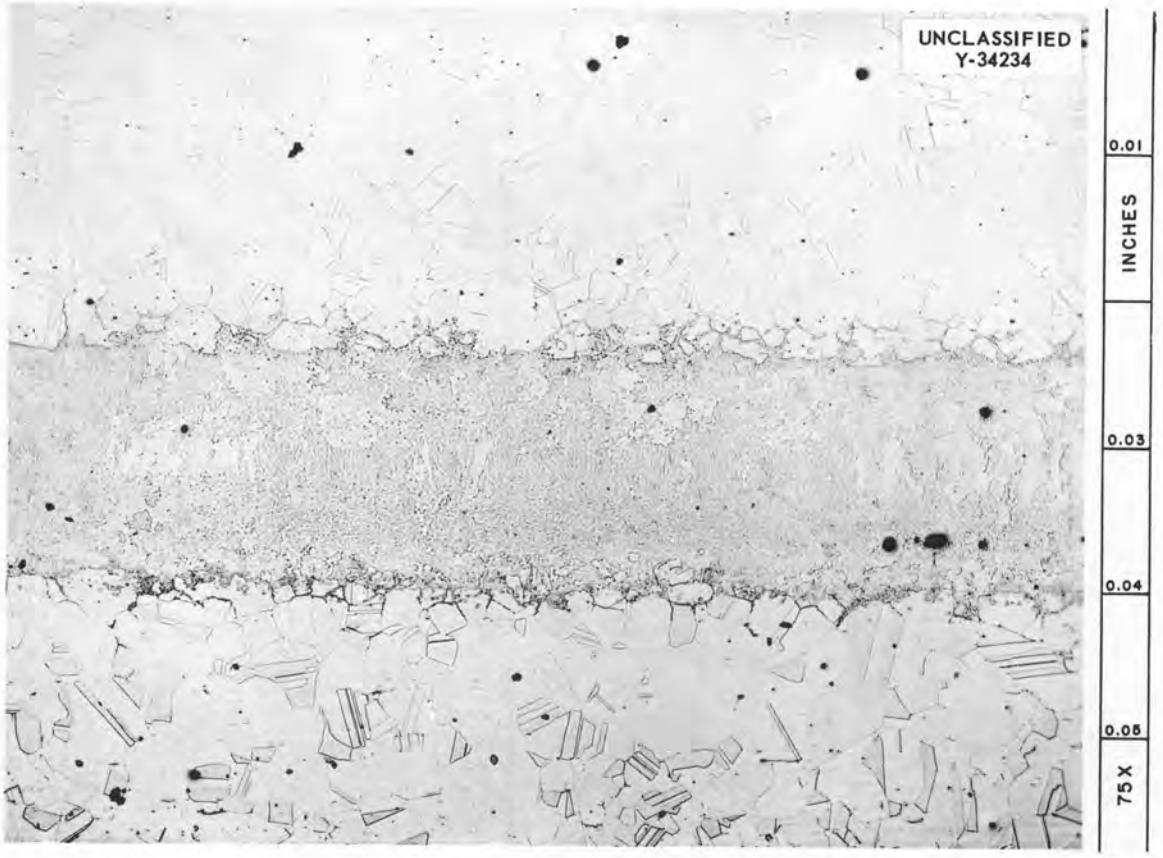

Fig. 4.17. Transverse Section of Spot Weld Between a 0.016-in.-Thick Type 304L Stainless Steel Cover Sheet and a 0.190-in.-Thick Type 304L Stainless Steel Frame Showing Character of Bond. Etchant: 5% CrO_3-electrolytic.

cycle. These clusters will be sent to the General Electric Vallecitos facility for examination. The other two clusters, identified as experiment 3, received irradiation during two 16-Mw ORR cycles and will receive further irradiation during an ORR 30-Mw cycle. The schedule is arranged to provide about twice as much burnup in experiment 3 as in experiment 1. It is anticipated that the peak burnup should be about 1700 Mwd/tonne of UO_2 for experiment 1 and over 3800 Mwd/tonne of UO_2 for experiment 3.

INTERNAL DISTRIBUTION

1. T. D. Anderson
2. V. E. Anderson (K-25)
3. S. E. Beall
4. R. J. Beaver
5. M. Bender
6. R. G. Berggren
7. D. S. Billington
8. R. E. Blanco
9. E. P. Blizard
10. T. V. Blosser
11. A. L. Boch
12. C. J. Borkowski
13. G. E. Boyd
14. E. J. Breeding
15. R. B. Briggs
16. F. R. Bruce
17. T. J. Burnett
18. D. W. Cardwell
19. C. E. Center (K-25)
20. R. A. Charpie
21. R. S. Cockreham
22. T. E. Cole
23. B. W. Colston
24. J. A. Conlin
25. W. B. Cottrell
26. J. A. Cox
27. F. L. Culler
28. H. N. Culver
29. J. E. Cunningham
30. I. T. Dudley
31. J. C. Ebersole
32. E. P. Epler
33. W. K. Ergen
34. B. R. Fish
35. A. P. Fraas
36. J. K. Franzreb
37. J. H. Frye, Jr.
38. W. R. Gall
39. B. L. Greenstreet
40. W. R. Grimes
41. E. E. Gross
42. J. C. Hart
43. V. O. Haynes
44. M. R. Hill
45. H. W. Hoffman
46. R. R. Holcomb
47. W. H. Jordan
48. S. I. Kaplan
49. P. R. Kasten
50. O. H. Klepper
51. R. B. Korsmeyer
52. P. G. Lafyatis
53. J. T. Lamartine
54. J. A. Lane
55. G. W. Leddicotte
56. R. N. Lyon
57. H. G. MacPherson
58. H. F. McDuffie
59. W. D. Manly
60. E. R. Mann
61. L. A. Mann
62. H. C. McCurdy
63. A. J. Miller
64. E. C. Miller
65. F. H. Neill
66. M. L. Nelson
67. W. R. Osborn
68. P. Patriarca
69. A. M. Perry
70. D. Phillips
71. P. M. Reyling
72. J. T. Roberts
73. M. W. Rosenthal
74. J. E. Rowe (K-25)
75. G. Samuels
76. H. W. Savage
77. A. W. Savolainen
78. L. D. Schaffer
79. O. Sisman
80. M. J. Skinner
81. G. M. Slaughter
82. A. H. Snell

83. I. Spiewak
84. P. E. Stein (Y-12)
85. J. A. Swartout
86. W. C. Thurber
87. D. E. Tidwell
88. D. B. Trauger
89. A. M. Weinberg
90. C. L. Whitmarsh
91. G. C. Williams
92. C. E. Winters
93. M. L. Winton
94-97. ORNL — Y-12 Technical Library Document Reference Section
98-109. Laboratory Records Department
110. Laboratory Records, ORNL R.C.
111-113. Central Research Library

EXTERNAL DISTRIBUTION

114-123. Division of Reactor Development (Maritime Reactors), AEC, Washington (Attn: R. P. Godwin)
124-125. Division of Reactor Development (Army Reactors), AEC, Washington (Attn: Col. G. B. Page)
126. Ebasco Services, Inc., New York (Attn: H. C. Ott)
127-129. New York Ship Building Corp., Camden, N. J. (Attn: M. W. Mann)
130-131. Research and Development Division, AEC, ORO
132-134. Reactor Division, AEC, ORO (Attn: D. F. Cope)
135-137. States Marine Lines, Inc. (Attn: R. D. Mehann)
138-139. The Babcock & Wilcox Company, Atomic Energy Division (Attn: D. W. Montgomery and R. T. Schomer)
140-716. Given distribution as shown in TID-4500 (15th ed.) under Reactors—Power category (75 copies — OTS)